

Electromagnetic properties of ${}^6\text{Li}$ in a cluster model with breathing clusters

A. T. Kruppa

*Magyar Tudományos Akadémia Atommagkutató Intézet, Debrecen, H-4001 Hungary
and Kernforschungszentrum Karlsruhe, Institut für Kernphysik III, D-7500 Karlsruhe 1, Federal Republic of Germany*

R. Beck* and F. Dickmann*

Kernforschungszentrum Karlsruhe, Institut für Kernphysik III, D-7500 Karlsruhe 1, Federal Republic of Germany

(Received 13 January 1987)

Electromagnetic properties of ${}^6\text{Li}$ are studied using a microscopic ($\alpha+d$) cluster model. In addition to the ground state of the clusters, their breathing excited states are included in the wave function in order to take into account the distortion of the clusters. The generator coordinate calculations are free from the spurious center-of-mass motion and arbitrary parameters. The cluster stability condition is satisfied. The elastic charge form factor F_{C0} is in good agreement with experiment up to momentum transfer 8 fm^{-2} . The discrepancy appearing at momentum transfer $q^2 > 8 \text{ fm}^{-2}$ must be attributed to the omission of the short range nucleon correlation. The ground state magnetic form factor F_{M1} and the inelastic charge form factor F_{C2}^* are also well described. The breathing excited states of d influence the behavior of F_{C0} at high momentum transfer only, but they have an effect on F_{M1} and F_{C2}^* even at low momentum transfer. The effect of the breathing states of α on the form factors proves to be negligible except at high momentum transfer. The ground-state charge density, rms charge radius, the magnetic dipole moment and a reduced transition strength are also obtained in fair agreement with experiment.

I. INTRODUCTION

It has been noted several times that among the p -shell nuclei ${}^6\text{Li}$ shows an anomalous behavior. In electron scattering the exceptional behavior of ${}^6\text{Li}$ appears in that its form factors cannot be described in the framework of the harmonic oscillator independent particle model consistently with the other p -shell nuclei.^{1,2} Attempts were made to describe the form factors of ${}^6\text{Li}$ by using different oscillator width parameters for the s - and p -shell nucleons,¹⁻³ configuration mixing,⁴⁻⁶ and a finite potential well for the average field.^{7,8} On the other hand, it turned out that the substantial residual two-body interaction present in ${}^6\text{Li}$ gives rise to short and long range correlation between the nucleons of ${}^6\text{Li}$.⁶⁻¹¹ Furthermore, ${}^6\text{Li}$ has proved to be one of the best cluster nuclei¹² and a huge amount of work has been devoted to understanding its cluster structure. It has been confirmed that the states of ${}^6\text{Li}$ can be interpreted in terms of an alpha (α) and a deuteron (d) cluster and the other two- and three-cluster structures play only a minor role.^{13,14}

The charge form factors of ${}^6\text{Li}$ have also been studied by an approach that differs essentially from the fully microscopic shell and cluster models. ${}^6\text{Li}$ was described by the motion of three structureless point particles, but the composite nature of α was approximately taken into account by the aid of Pauli-forbidden states.^{15,16} The three body problem was solved variationally or the exact Fadeev equations were considered.

In a previous paper¹⁷ we introduced a cluster model in which the distortion effects of the clusters were studied by using a generator coordinate (GC)-type trial wave function in which, in addition to the intercluster separation,

the oscillator width parameters of the clusters are treated as GC's. This amounts to improving the description of the ground states of the clusters and including, in the model, their breathing excitations. The specific (i.e., non-Pauli) distortion of the clusters is particularly important in an ($\alpha+d$)-type cluster model description since the loosely bound deuteron cluster can easily be distorted.

The effect of the specific distortion of the deuteron has been thoroughly investigated in the αd elastic scattering process.¹⁸⁻²⁵ However, there are relatively few papers concerned with similar analyses of the electromagnetic properties of the bound $\alpha+d$ system. Since the pioneering work of Kudiyarov *et al.*,²⁶ nondynamical microscopic harmonic oscillator cluster models have been widely used in the description of electron scattering from ${}^6\text{Li}$.²⁷⁻³¹ Such a consistent phenomenological approach has been recently developed.³² In this work the original cluster model has been modified such as to allow the deuteron to be deformed. In spite of the success of the phenomenological description, better understanding of the structure of ${}^6\text{Li}$ requires dynamical cluster models, i.e., cluster models based on the nucleon-nucleon (NN) interaction. Having solved the equation of motion for the approximate wave function, we may turn to the calculation of the matrix element of the electromagnetic multipole operators. Dynamically determined cluster model wave functions were used in Refs. 23, 24, and 33-37 in the calculation of electromagnetic properties of ${}^6\text{Li}$. However, in these calculations the α particle is kept undistorted and for the deuteron only a few excited states are included. In Ref. 23 it was pointed out that "one must obviously try to calculate with a more flexible deuteron wave function."

In this work our aim is to study the effect of reasonably complete sets of breathing excited states of both the alpha and the deuteron cluster on the electromagnetic properties of ${}^6\text{Li}$. Essentially similar calculations have recently been published for ${}^7\text{Li}$.^{38,39} The ground state properties we calculated are the charge monopole and the magnetic dipole form factors, the charge density distribution, and rms charge radius, while the calculated excitation properties are the reduced transition strength and the inelastic charge quadrupole form factor for the transition leading to the first excited state of ${}^6\text{Li}$.

The structure of the paper is the following. In the next section the cluster model with breathing clusters as applied to ${}^6\text{Li}$ is briefly reviewed. In Sec. III some standard formulas of the theory of the electron scattering are summarized and the procedure of calculating the GC kernels of the electromagnetic multipole operators is shown. The numerical results for the free clusters as well as for ${}^6\text{Li}$ are presented in Sec. IV.

II. BREATHING CLUSTER MODEL OF ${}^6\text{Li}$

The cluster model wave function of ${}^6\text{Li}$ is constructed from harmonic oscillator shell model states of the constituent clusters. The Slater determinant of the lowest shell model configuration of cluster c ($c = \alpha$ or d).

$$\Phi_c(M_c, \beta_c) = \mathcal{A}_c \left[\prod_{i=1}^{A_c} \phi(\mathbf{r}_i, \beta_c) \Sigma_c \right], \quad (2.1)$$

contains harmonic oscillator single-particle orbits of width parameter β_c

$$\phi(\mathbf{r}, \beta) = \left(\frac{\beta}{\pi} \right)^{3/4} \exp(-\beta \mathbf{r}^2 / 2) \quad (2.2)$$

and appropriate spin-isospin function Σ_c . The symbol M_c is the z component of the cluster spin angular momentum. The fixed quantum numbers of the clusters (total angular momentum, orbital momentum, spin and isospin) are suppressed for brevity. The antisymmetrization operator of the system c containing A_c nucleons is, in obvious notation,

$$\mathcal{A}_c = \frac{1}{(A_c!)^{1/2}} \sum_{\epsilon} (-)^{\epsilon} P_{\epsilon}. \quad (2.3)$$

In our GC method an unprojected basis function of ${}^6\text{Li}$ reads

$$\Psi(\beta_{\alpha}, \beta_d, \mathbf{s}, \mathbf{S}) = \mathcal{A}_{\alpha d} [\Phi_{\alpha}(\beta_{\alpha}, \mathbf{s}_{\alpha}) \Phi_d(\beta_d, \mathbf{s}_d)], \quad (2.4)$$

where the internuclear antisymmetrizer is

$$\mathcal{A}_{\alpha d} = \left[\frac{A_{\alpha}! A_d!}{(A_{\alpha} + A_d)!} \right]^{1/2} \left[1 + \sum_{\epsilon} (-)^{\epsilon} P_{\epsilon} \right] \quad (2.5)$$

and P_{ϵ} is a permutation operator between α and d . The form of the wave functions $\Phi_c(\beta_c, \mathbf{s}_c)$ is similar to Eq. (2.1):

$$\Phi_c(\beta_c, \mathbf{s}_c) = \mathcal{A}_c \left[\prod_{i=1}^{A_c} \phi(\mathbf{r}_i, \beta_c, \mathbf{s}_c) \Sigma_c \right], \quad (2.6)$$

but the harmonic oscillator orbits involved are centered at \mathbf{s}_c instead of the origin:

$$\phi(\mathbf{r}, \beta, \mathbf{s}) = \left(\frac{\beta}{\pi} \right)^{3/4} \exp[-\beta(\mathbf{r} - \mathbf{s})^2 / 2]. \quad (2.7)$$

In Eq. (2.4) we used the relative and average position vector of the oscillator centers,

$$\begin{aligned} \mathbf{s} &= \mathbf{s}_{\alpha} - \mathbf{s}_d, \\ \mathbf{S} &= \frac{1}{A_{\alpha} + A_d} (A_{\alpha} \mathbf{s}_{\alpha} + A_d \mathbf{s}_d). \end{aligned} \quad (2.8)$$

To proceed, we define translational invariant states. The projecting of internal states $\Phi_c^{\text{int}}(M_c, \beta_c)$ out of the wave function (2.1) is unambiguous. To get intrinsic states from (2.4), integration over \mathbf{S} is chosen,⁴⁰

$$\Psi^{\text{int}}(M_{\alpha} M_d, \beta_{\alpha}, \beta_d, \mathbf{s}) = \int d\mathbf{S} \Psi(\beta_{\alpha}, \beta_d, \mathbf{s}, \mathbf{S}). \quad (2.9)$$

The function (2.9) may be written in a form imitating the resonating group ansatz,

$$\begin{aligned} \Psi^{\text{int}}(M_{\alpha} M_d, \beta_{\alpha}, \beta_d, \mathbf{s}) \\ = \mathcal{A}_{\alpha d} [\Phi_{\alpha}^{\text{int}}(M_{\alpha}, \beta_{\alpha}) \Phi_d^{\text{int}}(M_d, \beta_d) \chi(\mathbf{R}_{\alpha d}, \beta_{\alpha}, \beta_d, \mathbf{s})], \end{aligned} \quad (2.10)$$

where the wave function of the relative motion is

$$\begin{aligned} \chi(\mathbf{R}_{\alpha d}, \beta_{\alpha}, \beta_d, \mathbf{s}) &= \left(\frac{\pi}{2\beta_{\alpha} + \beta_d} \right)^{3/2} \\ &\times \exp \left[-\frac{1}{2} \frac{4\beta_{\alpha}\beta_d}{2\beta_{\alpha} + \beta_d} (\mathbf{R}_{\alpha d} - \mathbf{s})^2 \right]. \end{aligned} \quad (2.11)$$

$\mathbf{R}_{\alpha d} = \mathbf{R}_{\alpha} - \mathbf{R}_d$ and \mathbf{R}_c is the center of mass of cluster c .

Finally, it remains to give the basis function of good total angular momentum \mathcal{FM} . First, the relative orbital angular momentum \mathcal{LM} between the α and d clusters is projected out by the help of the method given in Refs. 17 and 41,

$$\begin{aligned} \Psi^{\text{int}}(\mathcal{LM}, M_{\alpha} M_d, \beta_{\alpha}, \beta_d, s) \\ = \int d\hat{\mathbf{s}} Y_{\mathcal{LM}}(\hat{\mathbf{s}}) \Psi^{\text{int}}(M_{\alpha} M_d, \beta_{\alpha}, \beta_d, \mathbf{s}). \end{aligned} \quad (2.12)$$

The total-angular-momentum-projected function emerges from the coupling of the orbital momentum \mathcal{L} with the spin of the deuteron, which is the total spin (I) of the system,

$$\begin{aligned} \Psi^{\text{int}}(\mathcal{FM}, \mathcal{L}, \beta_{\alpha}, \beta_d, s) \\ = \sum_{M_d, \mathcal{M}} \langle \mathcal{LM} 1 M_d | \mathcal{FM} \rangle \Psi^{\text{int}}(\mathcal{LM}, M_{\alpha} M_d, \beta_{\alpha}, \beta_d, s). \end{aligned} \quad (2.13)$$

The wave function (2.13) is viewed as a generating function with s as well as β_{α} and β_d being the generator coordinates. So the trial wave function of ${}^6\text{Li}$ looks like

$$\Psi^{\text{int}}(\mathcal{FML}) = \int_0^\infty d\beta_\alpha \int_0^\infty d\beta_d \int_0^\infty ds f(\mathcal{FML}, \beta_\alpha, \beta_d, s) N(\beta_\alpha, \beta_d, s, \beta'_\alpha, \beta'_d, s') \times \Psi^{\text{int}}(\mathcal{FML}, \beta_\alpha, \beta_d, s). \quad (2.14)$$

$$N(\beta_\alpha, \beta_d, s, \beta'_\alpha, \beta'_d, s') = \langle \Psi^{\text{int}}(\mathcal{FML}, \beta_\alpha, \beta_d, s) | \Psi^{\text{int}}(\mathcal{FML}, \beta'_\alpha, \beta'_d, s') \rangle .$$

The GC amplitudes $f(\mathcal{FML}, \beta_\alpha, \beta_d, s)$ of Eq. (2.14) are determined by the variational principle

$$\delta E = \delta(\langle \Psi^{\text{int}} | H | \Psi^{\text{int}} \rangle / \langle \Psi^{\text{int}} | \Psi^{\text{int}} \rangle), \quad (2.15)$$

where the Hamiltonian has the form

$$H = -\frac{\hbar^2}{2M} \sum_i \Delta_{\mathbf{r}_i} + \sum_{i < j} V_{ij}(\mathbf{r}_i - \mathbf{r}_j) - T_{\text{c.m.}}. \quad (2.16)$$

Here, V_{ij} stands for the NN interactions and $T_{\text{c.m.}}$ is the kinetic energy operator of the center of mass. Using the ansatz (2.14) in Eq. (2.15), we get the Griffin-Hill-Wheeler integral equations.

$$\int_0^\infty d\beta'_\alpha \int_0^\infty d\beta'_d \int_0^\infty ds' [H(\beta_\alpha, \beta_d, s, \beta'_\alpha, \beta'_d, s') - EN(\beta_\alpha, \beta_d, s, \beta'_\alpha, \beta'_d, s')] f(\mathcal{FML}, \beta'_\alpha, \beta'_d, s') = 0, \quad (2.17)$$

where the Hamiltonian and overlap kernels are

$$H(\beta_\alpha, \beta_d, s, \beta'_\alpha, \beta'_d, s') = \langle \Psi^{\text{int}}(\mathcal{FML}, \beta_\alpha, \beta_d, s) | H | \Psi^{\text{int}}(\mathcal{FML}, \beta'_\alpha, \beta'_d, s') \rangle, \quad (2.18)$$

In the calculation the GC coordinates β_α and β_d are discretized, which means that in Eq. (2.14) the integrations over β_α and β_d are to be changed to summations over the discretization points, and, instead of $f(\mathcal{FML}, \beta_\alpha, \beta_d, s)$, the GC amplitudes $f_{ij}(\mathcal{FML}, s)$ have to be used (and in what follows will be used) corresponding to the discretization $\{\beta_\alpha^i\}_{i=1, \dots, N_\alpha}$ and $\{\beta_d^j\}_{j=1, \dots, N_d}$. We can proceed with a few number of discretization points provided their values are carefully selected. Here they are determined by the stability condition, for the free clusters, whose importance is emphasized in the literature.³⁹ The wave function of the free cluster c is taken in the following form:

$$\Psi_c^{(p)}(M_c) = \sum_{i=1}^{N_c} f_c^{p,i} \Phi_c^{\text{int}}(M_c, \beta_c^i). \quad (2.19)$$

The symbol p distinguishes different orthogonal states of c ($p=1$ corresponds to the ground state). The widths β_c^i and amplitudes $f_c^{p,i}$ are determined by minimizing the energy mean value of the c -cluster Hamiltonian. These optimum values of β_c^i are adopted for ${}^6\text{Li}$ as well.

Using the cluster states (2.19), the trial wave function (2.14) can be written in a more physical form,

$$\Psi^{\text{int}}(\mathcal{FML}) = \sum_{p=1}^{N_\alpha} \sum_{q=1}^{N_d} \sum_{M_\alpha, M_d} \langle \mathcal{L} M_\alpha M_d | \mathcal{FM} \rangle \mathcal{A}_{\alpha d} [\Psi_\alpha^{(p)}(M_\alpha) \Psi_d^{(q)}(M_d) \chi(\mathbf{R}_{\alpha d}, \mathcal{FML})_{p,q}], \quad (2.20)$$

$$\chi(\mathbf{R}_{\alpha d}, \mathcal{FML})_{p,q} = \sum_{i=1}^{N_\alpha} \sum_{j=1}^{N_d} t_\alpha^{i,p} t_d^{j,q} \int_0^\infty ds f_{ij}(\mathcal{FML}, s) \int d\hat{s} Y_{\mathcal{L}, \mathcal{M}}(\hat{s}) \chi(\mathbf{R}_{\alpha d}, \beta_\alpha^i, \beta_d^j, \mathbf{s}), \quad (2.21)$$

and the coefficients $t_c^{i,p}$ arise from the inversion of Eq. (2.19), i.e.,

$$\Phi_c^{\text{int}}(M_c, \beta_c^i) = \sum_{p=1}^{N_c} t_c^{i,p} \Psi_c^{(p)}(M_c). \quad (2.22)$$

This inversion is always possible because of the fact that the functions $\{\Phi_c^{\text{int}}(M_c, \beta_c^i)\}_{i=1, \dots, N_c}$ are linearly independent, the cluster states $\{\Psi_c^{(p)}(M_c)\}_{p=1, \dots, N_c}$ are orthogonal by construction, and both sets span the same subspace.

In addition to the ground state, the ansatz (2.19) produces $N_c - 1$ pseudostates, which may be interpreted as the breathing modes. In the case of the α particle, the first excited model state may be identified with the actually observed breathing mode at an excitation energy 20.1 MeV.

The inclusion of the excited cluster states in the sum (2.20) may take into account the specific distortion effects of the clusters. We will denote this model by $D_\alpha D_d$ (D standing for distortion). In order to study the influence of

the cluster distortion, restricted calculations were also carried out, in which we simply “switch off” the cluster distortion. Here we do this for the α (d) cluster by making the following ansatz for the GC amplitude

$$f_{ij}(s) = f_{\alpha(d)}^{1,i(j)} f_{j(i)}^{d(\alpha)}(s),$$

where the $f_{\alpha(d)}^{1,i(j)}$ are the known GC amplitudes of the ground state of the free α (d); the remaining parts, $f_{j(i)}^{d(\alpha)}(s)$, are determined variationally. We may also switch off all distortion using the ansatz $f_{ij}(s) = f_\alpha^{1,i} f_d^{j,j}$ and calculate $f(s)$ variationally. We will denote the restricted calculations by $G_\alpha D_d$, $G_\alpha G_d$, and $D_\alpha G_d$ (G standing for ground state). In these models, one or both of the clusters are only represented by their ground states.

In addition to these models, called many-width (MW) models, two simpler models are also considered: that in which the clusters have one common width (CW) parameter and that in which the clusters have two different single width (DW) parameters. In the first case the common

width parameter is selected by minimizing the sum of the intrinsic energies of α and d .

In order to study the force dependence of the results, three effective central NN interactions were employed: the Volkov force No. 2 (V2),⁴² the Brink-Boeker force B1 (BB1),⁴³ given in the form

$$V_{ij}(\mathbf{r}_i - \mathbf{r}_j) = \sum_k V_k(\mathbf{r}_i - \mathbf{r}_j)(W_k + M_k P_r + B_k P_\sigma - H_k P_\tau), \quad (2.23)$$

and the central part of the Minnesota force⁴⁴ (MN), which has the form

$$V_{ij}(\mathbf{r}_i - \mathbf{r}_j) = [V_R(\mathbf{r}_i - \mathbf{r}_j) + \frac{1}{2}V_i(\mathbf{r}_i - \mathbf{r}_j)(1 + P_\sigma) + \frac{1}{2}V_s(\mathbf{r}_i - \mathbf{r}_j)(1 - P_\sigma)][\frac{1}{2}u + \frac{1}{2}(2 - u)]P_r, \quad (2.24)$$

where P_r , P_σ , and P_τ are the space, spin, and isospin exchange operators, respectively, and we set $W_k + M_k + B_k + H_k = 1$. The spatial dependence of the nucleon-nucleon interaction used is pure Gaussian. The Coulomb interaction is taken into account by a Gaussian expansion.⁴⁵

III. GENERATOR COORDINATE DESCRIPTION OF ELECTROMAGNETIC PROPERTIES

A. Formulas of the theory of electron scattering

In a plane-wave Born approximation, neglecting the electron mass, the cross section for unpolarized electron

scattering from a nucleus with mass M_t may be written^{46,47} as

$$\sigma(\theta) = \frac{\sigma_M}{1 + \frac{2E}{M_t c^2} \sin^2 \theta / 2} \times \left[\frac{q_\mu^4}{q^4} F_L^2(q^2) + \left[\frac{1}{2} \frac{q_\mu^2}{q^2} + \tanh^2 \frac{\theta}{2} \right] F_T^2(q^2) \right], \quad (3.1)$$

where θ is the scattering angle and the Mott cross section

$$\sigma_M = \left[\frac{Ze}{2E} \right]^2 \frac{\cos^2 \theta / 2}{\sin^4 \theta / 2} \quad (3.2)$$

describes electron scattering from the Coulomb field of a point charge Ze . The quantity

$$q_\mu = (p_\mu - p'_\mu) / \hbar = (\omega / \hbar c, \mathbf{q})$$

is the four-momentum transfer divided by \hbar , where the incident and scattered four-momenta of the electron are $p_\mu = (E/c, \mathbf{p})$ and $p'_\mu = (E'/c, \mathbf{p}')$. The longitudinal and transverse form factors $F_L^2(q^2)$ and $F_T^2(q^2)$ can be expanded in terms of multipole components,

$$F_L^2(q^2) = \sum_{\lambda=0}^{\infty} |F_{C\lambda}(q)|^2 = \frac{1}{2\mathcal{F}_i + 1} \frac{4\pi}{Z^2} \sum_{\lambda=0}^{\infty} |\langle \mathcal{F}_f \| T_\lambda^C(q) \| \mathcal{F}_i \rangle|^2 \quad (3.3)$$

and

$$F_T^2(q^2) = \sum_{\lambda=1}^{\infty} [|F_{M\lambda}(q)|^2 + |F_{E\lambda}(q)|^2] = \frac{1}{2\mathcal{F}_i + 1} \frac{4\pi}{Z^2} \sum_{\lambda=1}^{\infty} [|\langle \mathcal{F}_f \| T_\lambda^M(q) \| \mathcal{F}_i \rangle|^2 + |\langle \mathcal{F}_f \| T_\lambda^E(q) \| \mathcal{F}_i \rangle|^2]. \quad (3.4)$$

here, $|\mathcal{F}_i\rangle$ and $|\mathcal{F}_f\rangle$ are the initial and final nuclear states with total angular momentum \mathcal{F}_i and \mathcal{F}_f , respectively.

The Coulomb, transverse magnetic, and transverse electric multipole operators are related to the charge and current density operators $\rho(\mathbf{r})$ and $\mathcal{F}(\mathbf{r})$ of the nucleus by

$$T_{\lambda\mu}^C(q) = \int d\mathbf{r} j_\lambda(qr) Y_{\lambda\mu}(\hat{\mathbf{r}}) \rho(\mathbf{r}), \quad (3.5)$$

$$T_{\lambda\mu}^E(q) = \frac{1}{q} \int d\mathbf{r} \nabla \times [j_\lambda(qr) \mathbf{Y}_{\lambda\lambda 1}^\mu(\mathbf{r})] \cdot \mathcal{F}(\mathbf{r}), \quad (3.6)$$

$$T_{\lambda\mu}^C(q) = \sum_i e_i j_\lambda(qr_i) Y_{\lambda\mu}(\hat{\mathbf{r}}_i), \quad (3.8)$$

$$T_{\lambda\mu}^M(q) = \sum_i \frac{i\hbar}{Mc} q \left\{ \left[- \left[\frac{\mathcal{F}}{2\mathcal{F}+1} \right]^{1/2} j_{\lambda+1}(qr_i) \mathbf{Y}_{\lambda\lambda+1}^\mu(\mathbf{r}_i) + \left[\frac{\mathcal{F}+1}{2\mathcal{F}+1} \right]^{1/2} j_{\lambda-1}(qr_i) \mathbf{Y}_{\lambda\lambda-1}^\mu(\mathbf{r}_i) \right] \frac{\mu_i}{2} \sigma(i) - j_\lambda(qr_i) \mathbf{Y}_{\lambda\lambda 1}^\mu(\mathbf{r}_i) \frac{e_i}{q} \nabla_{\mathbf{r}_i} \right\}, \quad (3.9)$$

and

and

$$T_{\lambda\mu}^M(q) = \int d\mathbf{r} j_\lambda(qr) \mathbf{Y}_{\lambda\lambda 1}^\mu(\mathbf{r}) \cdot \mathcal{F}(\mathbf{r}), \quad (3.7)$$

where j_λ , $Y_{\lambda\mu}$, and $\mathbf{Y}_{\lambda\lambda 1}^\mu$ are the spherical Bessel function, spherical harmonics, and vector spherical harmonics, respectively. If the charge and current density operators of the nucleus are taken to be sums of the corresponding free densities of point-like nucleons, the multipole operators become

$$T_{\lambda\mu}^E(q) = \sum_i \frac{\hbar}{Mc} q \left\{ \left[- \left(\frac{\mathcal{F}}{2\mathcal{F}+1} \right)^{1/2} j_{\lambda+1}(qr_i) \mathbf{Y}_{\lambda\lambda+1}^{\mu}(\mathbf{r}_i) + \left(\frac{\mathcal{F}+1}{2\mathcal{F}+1} \right)^{1/2} j_{\lambda-1}(qr_i) \mathbf{Y}_{\lambda\lambda-1}^{\mu}(\mathbf{r}_i) \right] \frac{e_i}{q} \nabla_{\mathbf{r}_i} + j_{\lambda}(qr_i) \mathbf{Y}_{\lambda\lambda}^{\mu}(\mathbf{r}_i) \frac{\mu_i}{2} \boldsymbol{\sigma}(i) \right\}, \quad (3.10)$$

where M is the nucleon mass, $e_i = \frac{1}{2}[1 + \tau_3(i)]$,

$$\mu_i = \frac{1}{2}[1 + \tau_3(i)]\mu_p + \frac{1}{2}[1 - \tau_3(i)]\mu_n, \quad \mu_p = 2.79, \quad \mu_n = -1.91$$

and the Pauli spin and isospin operators of the i th nucleon are $\boldsymbol{\sigma}(i)$ and $\boldsymbol{\tau}(i)$. The finite size effect of the proton can be taken into account by multiplication by the appropriate proton form factor. The charge form factor of the proton may be approximated⁴⁷ by

$$\exp(-a_p^2 q^2/4), \quad a_p^2 = 0.43 \text{ fm}^{-2}. \quad (3.11)$$

By studying the low momentum transfer behavior of the form factors, further electromagnetic observables can be deduced. In elastic scattering ($\mathcal{F}_i = \mathcal{F}_f = \mathcal{F}$) the multipole expansion of the total charge form factor is given by

$$F_L^E(q^2) = F_{C0}(q^2)^2 + \frac{1}{180} \left(\frac{Q^2 q^4}{Z^2} \right) \frac{1}{(2\mathcal{F}+1) \begin{bmatrix} \mathcal{F} & 2 & \mathcal{F} \\ -\mathcal{F} & 0 & \mathcal{F} \end{bmatrix}^2} + \dots, \quad (3.12)$$

where $F_{C0}(q^2)$ is the electric monopole form factor and Q is the electric quadrupole moment. For $q \rightarrow 0$, the monopole form factor may be expanded as

$$F_{C0}(q^2)^2 = (1 - \frac{1}{6}\langle r^2 \rangle q^2 + \frac{1}{120}\langle r^4 \rangle q^4 + \dots)^2, \quad (3.13)$$

where $\langle r^2 \rangle$ is the mean square radius:

$$\langle r^2 \rangle = -3 \left. \frac{d^2 F_{C0}}{dq^2} \right|_{q=0}. \quad (3.14)$$

From the behavior of the transverse form factor in the long wavelength limit, the ground state magnetic dipole moment can be obtained as

$$\mu^2 = 3 \left[\frac{\mathcal{F}}{\mathcal{F}+1} \right] \left[\frac{ZMc}{\hbar} \right]^2 \left. \frac{d^2 F_T^2}{dq^2} \right|_{q=0}, \quad (3.15)$$

where μ is expressed in units of the nuclear magneton μ_N . In the long wavelength limit the reduced matrix element of the Coulomb multipole operator is related to the radiative decay lifetime τ_{λ} by

$$\tau_{\lambda}^{-1} = \frac{8\pi(\lambda+1)}{\lambda[(2\lambda+1)!!]^2} \frac{1}{\hbar} \left[\frac{E_x}{\hbar c} \right]^{2\lambda+1} B(E\lambda, \mathcal{F}_i \rightarrow \mathcal{F}_f), \quad (3.16)$$

where the reduced transition strength is

$$B(E\lambda, \mathcal{F}_i \rightarrow \mathcal{F}_f) = \frac{1}{q \rightarrow 0} \frac{1}{2\mathcal{F}_i+1} \left[\frac{(2\lambda+1)!!}{q^{\lambda}} \right]^2 \times |\langle \mathcal{F}_f || T_{\lambda}^C(q) || \mathcal{F}_i \rangle|^2. \quad (3.17)$$

Following Uberall,⁴⁸ the transition charge density is defined by

$$\rho_{if}^{\lambda}(r) = \langle \mathcal{F}_f || \rho_{\lambda}(r) || \mathcal{F}_i \rangle, \quad (3.18)$$

where

$$\rho_{\lambda\mu}(r) = \int d\hat{\mathbf{r}} Y_{\lambda\mu}(\hat{\mathbf{r}}) \rho(\mathbf{r}). \quad (3.19)$$

The multipole component of the charge form factor can be expressed in terms of the transition charge density as

$$F_{C\lambda}(q) = \frac{(4\pi)^{1/2}}{Z(2\mathcal{F}_i+1)^{1/2}} \int_0^{\infty} dr j_{\lambda}(qr) \rho_{if}^{\lambda}(r). \quad (3.20)$$

Inversion of Eq. (3.20) gives

$$\rho_{if}^{\lambda}(r) = \frac{Z(2\mathcal{F}_i+1)^{1/2}}{\pi^{3/2}} \int_0^{\infty} dq j_{\lambda}(qr) F_{C\lambda}(q). \quad (3.21)$$

B. Generator coordinate kernels of the electromagnetic multipole operators

To evaluate electromagnetic quantities in the framework of the GC method, we need the GC kernels of the electromagnetic multipole operators. In the following the calculation of the longitudinal form factor is sketched and the magnetic dipole form factor of the ground state is shown.

In the calculation of the charge form factor the center-of-mass motion has to be treated correctly^{49,50} since this motion may have a great influence on the charge form factor at high momentum transfer. Of course, using the wave function (2.14) composed of the internal states (2.9), we do not face the problem of the center-of-mass motion, but a new difficulty arises. The calculation of the matrix elements of electromagnetic multipole operators in terms of internal wave functions, which are not Slater determinants, is very complicated. A way to overcome this difficulty is to keep all single particle coordinates and to use the wave function

$$\Psi_{\mathbf{K}}(\mathcal{F}\mathcal{M}\mathcal{L}) = \frac{1}{(2\pi)^{3/2}} \exp(i\mathbf{K} \cdot \mathbf{R}_{\text{c.m.}}) \Psi^{\text{int}}(\mathcal{F}\mathcal{M}\mathcal{L}). \quad (3.22)$$

The plane wave describing the center-of-mass motion can be incorporated in the single particle orbits. The function

$\Psi_{\mathbf{K}}(\mathcal{F}\mathcal{M}\mathcal{L})$ is then to be constructed from single particle orbits,

$$\phi_{\mathbf{K}}(\mathbf{r}, \beta, \mathbf{s}) = \frac{1}{(2\pi)^{3/2(A_\alpha + A_d)}} \left[\frac{\beta}{\pi} \right]^{3/4} \times \exp[i\mathbf{K} \cdot \mathbf{r} / (A_\alpha + A_d) - \beta(\mathbf{r} - \mathbf{s})^2 / 2], \quad (3.23)$$

just as $\Psi(\mathcal{F}\mathcal{M}\mathcal{L})$ is constructed from $\phi(\mathbf{r}, \beta, \mathbf{s})$ of (2.7). When the cluster width parameters are equal, the cumbersome linear momentum projection can be avoided by taking into account the Tassie-Barker correction⁵¹ in the charge form factor.

With the definitions of Sec. II, the wave function (3.22) can be cast into the form

$$\Psi_{\mathbf{K}}(\mathcal{F}\mathcal{M}\mathcal{L}) = \sum_{i=1}^{N_\alpha} \sum_{j=1}^{N_d} \sum_{M_d} \langle \mathcal{L}\mathcal{M}1M_d | \mathcal{F}\mathcal{M} \rangle \int_0^\infty ds f_{ij}(\mathcal{F}\mathcal{M}\mathcal{L}, s) \int d\hat{\mathbf{s}} Y_{\mathcal{L}\mathcal{M}}(\hat{\mathbf{s}}) \int d\mathbf{S} \Psi_{\mathbf{K}}(\beta_\alpha^i, \beta_d^j, \mathbf{s}, \mathbf{S}), \quad (3.24)$$

where

$$\Psi_{\mathbf{K}}(\beta_\alpha, \beta_d, \mathbf{s}, \mathbf{S}) = \mathcal{A}_{\alpha d} \left[\prod_{i \in \alpha} \phi_{\mathbf{K}}(\mathbf{r}_i, \beta_\alpha, \mathbf{s}_\alpha) \prod_{j \in d} \phi_{\mathbf{K}}(\mathbf{r}_j, \beta_d, \mathbf{s}_d) \Sigma_\alpha \Sigma_d \right]. \quad (3.25)$$

The reduced matrix element of an irreducible tensor operator $O_{\lambda\mu}$ of rank λ between initial and final states of the form (3.24) can be written as

$$\langle \Psi_{\mathbf{K}_f}(\mathcal{F}_f \mathcal{L}_f) | O_\lambda | \Psi_{\mathbf{K}_i}(\mathcal{F}_i \mathcal{L}_i) \rangle = \sum_{i,i'=1}^{N_\alpha} \sum_{j,j'=1}^{N_d} \int_0^\infty ds f_{ij}(\mathcal{F}_f \mathcal{L}_f, s)^* \int_0^\infty ds' f_{i'j'}(\mathcal{F}_i \mathcal{L}_i, s') \{ O \}_{ij,i'j'}^{\text{AMP}}(s, s'), \quad (3.26)$$

where the angular-momentum-projected (AMP) kernel of $O_{\lambda\mu}$ is defined by

$$\{ O \}_{ij,i'j'}^{\text{AMP}}(s, s') = \sum_{M_d, M_d'} \sum_{M_d'} (-)^{M_i - \mathcal{F}_i} \langle \mathcal{L}_f \mathcal{M}_f 1 M_d | \mathcal{F}_f \mathcal{M}_f \rangle \langle \mathcal{L}_i \mathcal{M}_i 1 M_d | \mathcal{F}_i \mathcal{M}_i \rangle \frac{1}{\langle \mathcal{F}_f \mathcal{M}_f \mathcal{F}_i - M_i | \lambda, \mu \rangle} \times \int d\hat{\mathbf{s}} Y_{\mathcal{L}_f \mathcal{M}_f}^*(\hat{\mathbf{s}}) \int d\hat{\mathbf{s}}' Y_{\mathcal{L}_i \mathcal{M}_i}(\hat{\mathbf{s}}') \{ O \}_{ij,i'j'}^{\text{LMP}}(\mathbf{s}, \mathbf{s}'), \quad (3.27)$$

and the linear-momentum-projected (LMP) kernel of $O_{\lambda\mu}$ is given in the form

$$\{ O \}_{ij,i'j'}^{\text{LMP}}(\mathbf{s}, \mathbf{s}') = \int d\mathbf{S} \int d\mathbf{S}' \langle \Psi_{\mathbf{K}_f}(\beta_\alpha^i, \beta_d^j, \mathbf{s}, \mathbf{S}) | O_{\lambda\mu} | \Psi_{\mathbf{K}_i}(\beta_\alpha^{i'}, \beta_d^{j'}, \mathbf{s}', \mathbf{S}') \rangle, \quad (3.28)$$

where $\hat{\mathbf{s}}$ and $\hat{\mathbf{s}}'$ denote the angle variables of the vectors \mathbf{s} and \mathbf{s}' . The integrand of Eq. (3.28) can be calculated straightforwardly due to the fact that the wave functions appearing in it are simple Slater determinants. Because of computational convenience, the Coulomb multipole operator given in Eq. (3.8) was rewritten in the form

$$T_{\lambda\mu}^C(q) = \sum_k e_k \frac{1}{4\pi i^\lambda} \int d\hat{\mathbf{q}} Y_{\lambda\mu}(\hat{\mathbf{q}}) \exp(i\mathbf{q} \cdot \mathbf{r}_k). \quad (3.29)$$

$$\{ T_{\lambda\mu}^C(q) \}_{ij,i'j'}^{\text{LMP}}(\mathbf{s}, \mathbf{s}') = \sum_{k=1}^6 \sum_{\epsilon} (-)^\epsilon M_\epsilon \exp(-b_{\epsilon,k} q^2 - u_\epsilon s^2 - u'_\epsilon s'^2 + w_\epsilon \mathbf{s} \cdot \mathbf{s}') \frac{e_k}{4\pi i^\lambda} \Delta_\epsilon \int d\hat{\mathbf{q}} Y_{\lambda\mu}(\hat{\mathbf{q}}) \exp(if_{\epsilon,k} \mathbf{q} \cdot \mathbf{s} + if'_{\epsilon,k} \mathbf{q} \cdot \mathbf{s}'), \quad (3.30)$$

where, in obvious notation,

$$\Delta_\epsilon = \delta_{1, \sigma_3(\epsilon_1)} \cdots \delta_{6, \sigma_3(\epsilon_6)} \delta_{1, \tau_3(\epsilon_1)} \cdots \delta_{6, \tau_3(\epsilon_6)} \quad (3.31)$$

originates from the inner products of the spin and isospin functions. The summations in Eq. (3.30) run over the indexes of the nucleons and permutations. The coefficients M_ϵ , $b_{\epsilon,k}$, u_ϵ , u'_ϵ , w_ϵ , $f_{\epsilon,k}$, $f'_{\epsilon,k}$ still depend on the cluster width parameters β_α^i , β_d^j , $\beta_\alpha^{i'}$, and $\beta_d^{j'}$. Out of $6 \times 6!$ terms of the sum in (3.30), only four different ones survive. The

In the following the wave function (3.24) is assumed to be normalized, i.e.,

$$\langle \Psi_{\mathbf{K}_f}(\mathcal{F}_f \mathcal{M}_f \mathcal{L}_f) | \Psi_{\mathbf{K}_i}(\mathcal{F}_i \mathcal{M}_i \mathcal{L}_i) \rangle = \delta(\mathbf{K}_i - \mathbf{K}_f),$$

and in the GC kernels the Dirac delta function $\delta(\mathbf{K}_i + \mathbf{q} - \mathbf{K}_f)$ expressing the conservation of the total linear momentum will be omitted.

A lengthy but straightforward calculation gives the linear-momentum-projected kernel of $T_{\lambda\mu}^C(q)$:

terms in (3.30) may be classified according to how many particles are exchanged between α and d and the manner in which the photon interacts with a particular nucleon in the clusters.⁵² Explicit expressions of the coefficients M_ϵ , $b_{\epsilon,k}$, u_ϵ , u'_ϵ , w_ϵ , $f_{\epsilon,k}$, $f'_{\epsilon,k}$ will be published elsewhere. Expanding the exponential function in (3.30) into spherical harmonics of the angles $\hat{\mathbf{s}}$ and $\hat{\mathbf{s}}'$, the integration indicated in Eq. (3.27) can easily be carried out, and after some angular momentum algebraic manipulation, the AMP kernel of $T_{\lambda\mu}^C(q)$ can be written in the form

$$\begin{aligned}
\{T_{\lambda}^C(q)\}_{ij,i'j'}^{\text{AMP}} &= (4\pi)^{1/2} \hat{\mathcal{L}}_i \hat{\mathcal{L}}_f \hat{\lambda} \sum_{\epsilon} \sum_{k=1}^6 \sum_{L,L',L''=0}^{\infty} i^{L+L'+\lambda} \hat{\mathcal{L}}^2 \hat{\mathcal{L}}'^2 \hat{\mathcal{L}}''^2 (-)^{L'+\lambda} \\
&\times \begin{bmatrix} \lambda & L & L' \\ 0 & 0 & 0 \end{bmatrix} \begin{bmatrix} \mathcal{L}_f & L & L'' \\ 0 & 0 & 0 \end{bmatrix} \begin{bmatrix} \mathcal{L}_i & L' & L'' \\ 0 & 0 & 0 \end{bmatrix} \\
&\times \begin{bmatrix} \mathcal{L}_f & \lambda & \mathcal{L}_i \\ L' & L'' & L \end{bmatrix} j_L(f_{\epsilon,k}qs) j_{L'}(f'_{\epsilon,k}qs') \\
&\times i_{L''}(w_{\epsilon}ss') \exp(-b_{\epsilon,k}q^2 - u_{\epsilon}s^2 - u'_{\epsilon}s'^2) (-)^{\epsilon} M_{\epsilon} \Delta_{\epsilon} e_k, \quad (3.32)
\end{aligned}$$

where i_L is the modified spherical harmonics of the first kind and $\hat{\mathcal{L}} = (2L + 1)^{1/2}$.

For elastic scattering, $\mathcal{F}_i = \mathcal{F}_f = 1$ and $\mathcal{L}_i = \mathcal{L}_f = 0$, the expression (3.32) becomes simpler. Using Eq. (3.3) the AMP kernel of the Coulomb monopole form factor emerges as

$$\begin{aligned}
\{F_{C0}(q^2)^2\}_{ij,i'j'}^{\text{AMP}} &= \left[\frac{4\pi}{3} \right]^2 \left| \sum_{\epsilon} \sum_{k=1}^6 \sum_{L=0}^{\infty} (-)^{\epsilon} M_{\epsilon} (-)^L (2L + 1) j_L(f_{\epsilon,k}qs) \right. \\
&\quad \left. \times j_L(f'_{\epsilon,k}qs') i_L(w_{\epsilon}ss') \exp(-b_{\epsilon,k}q^2 - u_{\epsilon}s^2 - u'_{\epsilon}s'^2) e_k \Delta_{\epsilon} \right|^2. \quad (3.33)
\end{aligned}$$

The AMP kernel of the mean square radius can be derived combining Eqs. (3.14) and (3.33):

$$\begin{aligned}
\{\langle r^2 \rangle\}_{ij,i'j'}^{\text{AMP}}(s,s') &= -4\pi \sum_{\epsilon} \sum_{k=1}^6 (-)^{\epsilon} M_{\epsilon} \exp(-u_{\epsilon}s^2 - u'_{\epsilon}s'^2) e_k \Delta_{\epsilon} \\
&\quad \times \left[i_0(w_{\epsilon}ss') (2b_{\epsilon,k} - \frac{1}{3}f_{\epsilon,k}^2s^2 - \frac{1}{3}f'_{\epsilon,k}{}^2s'^2) - \frac{2}{3}i_1(w_{\epsilon}ss') f_{\epsilon,k} f'_{\epsilon,k} ss' \right]. \quad (3.34)
\end{aligned}$$

According to Eq. (3.21), the charge density of the ground state is the Fourier transform of the charge form factor F_{C0} . This transformation was done numerically in the actual calculation.

The charge form factor F_{C2}^* of the inelastic electron scattering leading to the first excited state of ${}^6\text{Li}$ can be obtained from the general results (3.32) and (3.3) by inserting the corresponding quantum numbers into these expressions. In our model the quantum numbers $\mathcal{L} = 0$ and 2 are assigned to the ground and first excited states of ${}^6\text{Li}$. The AMP kernel of $F_{C2}^*(q)^2$ reads

$$\begin{aligned}
\{F_{C2}^*(q)^2\}_{ij,i'j'}^{\text{AMP}}(s,s') &= \frac{112\pi^2}{27} \left| \sum_{\epsilon} \sum_{k=1}^6 \sum_{L=0}^{\infty} \sum_{L'=|L-2|}^{L+2} (-)^{\epsilon} M_{\epsilon} e_k i^{L+L'} \Delta_{\epsilon} \hat{\mathcal{L}}^2 \hat{\mathcal{L}}'^2 \begin{bmatrix} 2 & L & L' \\ 0 & 0 & 0 \end{bmatrix} \right. \\
&\quad \left. \times \exp(-b_{\epsilon,k}q^2 - u_{\epsilon}s^2 - u'_{\epsilon}s'^2) j_L(f_{\epsilon,k}qs) j_{L'}(f'_{\epsilon,k}qs') i_{L'}(w_{\epsilon}ss') \right|^2. \quad (3.35)
\end{aligned}$$

Substituting expression (3.35) into Eq. (3.17) and taking the limit $q \rightarrow 0$, we obtain the general formula of the electric 2^{λ} pole reduced transition strength,

$$\begin{aligned}
\{B(E\lambda, \mathcal{F}_i \rightarrow \mathcal{F}_f)\}_{ij,i'j'}^{\text{AMP}}(s,s') &= \hat{\mathcal{F}}_f^2 [(2\lambda + 1)!!]^2 \hat{\mathcal{L}}_i^2 \hat{\mathcal{L}}_f^2 \hat{\lambda}^2 \begin{Bmatrix} \mathcal{L}_f & \mathcal{F}_f & I \\ \mathcal{F}_i & \mathcal{L}_i & \lambda \end{Bmatrix} (-)^{2(\mathcal{F}_i + I)} (4\pi) \\
&\quad \times \left| \sum_{\epsilon} \sum_{k=1}^6 \sum_{L,L',L''=0}^{\infty} (-)^{\epsilon} M_{\epsilon} i^{L+L'+\lambda} (-)^{L'+\lambda} \delta_{L+L',2L} \hat{\mathcal{L}}^2 \hat{\mathcal{L}}'^2 \hat{\mathcal{L}}''^2 \exp(-u_{\epsilon}s^2 - u'_{\epsilon}s'^2) e_k \Delta_{\epsilon} \right. \\
&\quad \times i_{L''}(w_{\epsilon}ss') (f_{\epsilon,k}s)^L (f'_{\epsilon,k}s')^{L'} \begin{bmatrix} \lambda & L & L' \\ 0 & 0 & 0 \end{bmatrix} \begin{bmatrix} \mathcal{L}_f & L' & L'' \\ 0 & 0 & 0 \end{bmatrix} \\
&\quad \left. \times \begin{bmatrix} \mathcal{L}_i & L' & L'' \\ 0 & 0 & 0 \end{bmatrix} \begin{bmatrix} \mathcal{L}_f & \lambda & \mathcal{L}_i \\ L' & L'' & L \end{bmatrix} [(2L + 1)!! (2L' + 1)!!]^{-1} \right|^2. \quad (3.36)
\end{aligned}$$

The specialization of the expression (3.36) for the transition $3^+ \rightarrow 1^+$ leads to

$$2100\pi \left| \sum_{\epsilon} \sum_{k=1}^6 \sum_{L,L'=0}^{\infty} i^{L+L'} \delta_{L+L',2} \hat{L}^2 \hat{L}'^2 (-)^{\epsilon} M_{\epsilon} \exp(-u_{\epsilon} s^2 - u'_{\epsilon} s'^2) i_{L'}(w_{\epsilon} s s') e_k \Delta_{\epsilon} \begin{pmatrix} 2 & L & L' \\ 0 & 0 & 0 \end{pmatrix}^2 \right. \\ \left. \times (f_{\epsilon,k} s)^L (f'_{\epsilon,k} s')^{L'} [(2L+1)!!(2L'+1)!!]^{-1} \right|^2. \quad (3.37)$$

We note in passing that Eqs. (3.32) and (3.36) are not restricted to ${}^6\text{Li}$. They are generally valid for any two s -wave cluster nucleus provided the summations over k and ϵ run over the nucleons and permutations involved by the particular nucleus. General expressions for the coefficients M_{ϵ} , $b_{\epsilon,k}$, u_{ϵ} , \dots can also be given. They depend on the mass number of the clusters and, of course, on the cluster width parameters.

After similar steps, the transverse magnetic dipole form factor F_{M1} of the ground state can be cast into the form

$$\{F_{M1}(q)^2\}_{ij,i'j'}^{\text{AMP}}(s,s') = \frac{64\pi^2}{27} \left[\frac{\hbar}{Mc} \right]^2 q^2 \left| \sum_{\epsilon} \sum_{k=1}^6 \sum_{L=0}^{\infty} (-)^{\epsilon} (-)^L \hat{L}^2 M_{\epsilon} \mu_k \sigma_k j_L(f_{\epsilon,k} q s) j_L(f'_{\epsilon,k} q s') i_L(w_{\epsilon} s s') \right. \\ \left. \times \exp(-b_{\epsilon,k} q^2 - u_{\epsilon} s^2 - u'_{\epsilon} s'^2) \Delta_{\epsilon} \right|^2, \quad (3.38)$$

where σ_k is $\frac{1}{2}$ for spin-up and $-\frac{1}{2}$ for spin-down states of the k 'th nucleon. It is worth mentioning that in the present model of ${}^6\text{Li}$ the convection current part of the current density operator happens to give a vanishing contribution to F_{M1} . After taking into account Eqs. (3.38) and (3.15), it turns out that the GC kernel of the ground state magnetic dipole moment μ is proportional to the norm kernel

$$\{\mu\}_{ij,i'j'}^{\text{AMP}}(s,s') = (\mu_p + \mu_n) N_{ij,i'j'}^{\text{AMP}}(s,s'), \quad (3.39)$$

where the norm kernel of the ground state is given by

$$N_{ij,i'j'}^{\text{AMP}}(s,s') = 4\pi \sum_{\epsilon} (-)^{\epsilon} M_{\epsilon} \\ \times \exp(-u_{\epsilon} s^2 - u'_{\epsilon} s'^2) i_0(w_{\epsilon} s s') \Delta_{\epsilon}. \quad (3.40)$$

The coefficients u_{ϵ} , u'_{ϵ} , w_{ϵ} , and M_{ϵ} in Eq. (3.30) are identical to those in the norm kernel (3.40). The consequence of Eq. (3.39) is that the magnetic dipole moment of the ground state, independent of the model and NN interaction used, is $\mu = 0.88 \mu_N$.

IV. RESULTS

A. Description of the free clusters

For the description of the ground state and breathing excited states of the free clusters, the intrinsic wave functions of the form (2.19) were used. In the MW model, to get a rough energy convergence within 1–2 keV it was enough to use three and five width parameters for α and d, respectively. They were determined by minimizing the microscopic cluster Hamiltonian. The optimum values of the widths are shown in Table I for the different models and interactions used.

In Table II the calculated and experimental values of the binding energies and root mean square (rms) radii of the clusters are displayed. The interactions V2 and BB1 are better for α than for d, while the MN force gives a

good description for d but fails for α . The rms radius of d is strikingly large in the MW model using the V2 or BB1 force. Direct numerical integrations of the Schrödinger equation of the deuteron, using the computer code GAMOW,⁵⁵ give virtually the same results as presented in Table II (e.g., the binding energies are -0.6083 , -1.0173 , and -2.2018 MeV for V2, BB1, and MN forces). Thus the MW model of d is essentially exact and adequate for the interactions used.

The ground state charge form factor of a nucleus with mass number less than five, assuming a normalized wave function of the form (2.19), may be written in the following form:

TABLE I. The oscillator width parameters of the clusters using different interactions and models. The cluster stability condition is satisfied in the DW and MW models.

		β_{α} (fm $^{-2}$)	β_d (fm $^{-2}$)
V2	CW	0.469	0.469
	DW	0.528	0.164
	MW	0.3159	0.0144, 0.7876
		0.6701	0.0602, 3.8191
	2.4367	0.23	
BB1	CW	0.461	0.461
	DW	0.503	0.162
	MW	0.3275	0.0233, 1.2075
		0.6971	0.0957, 5.0659
1.8139		0.3596	
MN	CW	0.582	0.582
	DW	0.606	0.4374
	MW	0.3534	0.0411, 1.6028
		0.7917	0.1511, 5.7864
2.6875		0.5151	

TABLE II. The binding energies (E_c) and rms radii ($\langle r_c^2 \rangle^{1/2}$) of the free clusters using different models and interactions. The experimental data are taken from Refs. 53 and 54.

		E_α (MeV)	$\langle r_\alpha^2 \rangle^{1/2}$ (fm)	E_d (MeV)	$\langle r_d^2 \rangle^{1/2}$ (fm)
V2	CW	-27.573	1.745	2.567	1.498
	DW	-27.957	1.666	0.579	2.284
	MW	-28.563	1.702	-0.608	3.530
BB1	CW	-27.097	1.757	2.523	1.507
	DW	-27.374	1.698	0.814	2.297
	MW	-28.460	1.702	-1.016	2.848
MN	CW	-24.633	1.606	0.189	1.391
	DW	-24.687	1.582	-0.1318	1.536
	MW	-25.595	1.620	-2.201	2.105
Expt.		-28.297	1.674 \pm 0.012	-2.225	2.095 \pm 0.006

$$|F_L(q^2)|^2 = 4\pi \left| \sum_{i,j=1}^{N_c} (f_c^{1,i})^* f_c^{1,j} \left[\frac{2\pi(\beta_c^i + \beta_c^j)}{A_c \beta_c^i \beta_c^j} \right]^{3/2} \left[\frac{4\beta_c^i \beta_c^j}{(\beta_c^i + \beta_c^j)^2} \right]^{3A_c/4} \exp\{-q^2(A_c - 1)/[2A_c(\beta_c^i + \beta_c^j)]\} \right|^2. \quad (4.1)$$

In Fig. 1 the measured values and some calculated elastic charge form factors of the α particle are shown as functions of the squared momentum transfer q^2 . In a single-width model the charge form factor depends only on the width parameter (independently of the interaction) and, according to expression (4.1), a diffraction dip cannot develop. In the MW model the calculated diffraction minima appear around $q^2 = 24.05$, 16.25, and 23.45 fm^{-2} for the V2, BB1, and MN interaction, respectively. The failure of the simple shell-model-type description to reproduce the diffraction dip is well known and it has

been shown that the short range correlation^{9,57} of the nucleons and meson exchange currents^{58,59} play substantial roles in the region of the minimum and the secondary maximum. In the small momentum transfer (SMT) region ($q^2 < 8 \text{ fm}^{-2}$) the best agreement with experiment was obtained by using the BB1 force. In spite of the fact that the rms radius of α is quite good with the MN interaction, the discrepancy in the binding energy also appears in the shape of the calculated charge form factor. In the MW model the charge form factor of α changes, with respect to the single width models, only very slightly

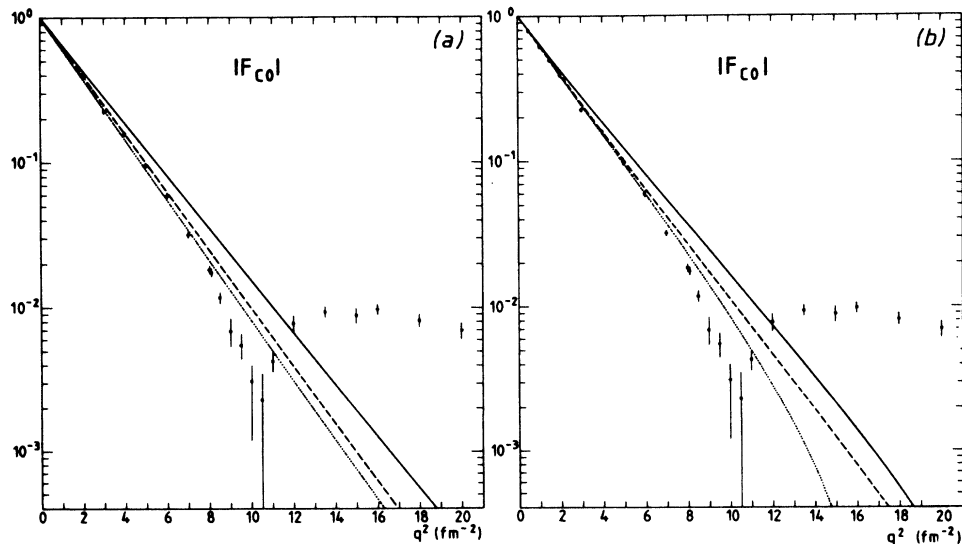


FIG. 1. Charge form factor of the ground state of the alpha particle: (a) in the DW model, (b) in the MW model. The solid, dashed, and dotted lines were calculated with the MN, V2, and BB1, interaction, respectively. The dots represent the data of Ref. 56.

in the SMT region.

For practical reasons the elastic electron-deuteron scattering cross sections is usually given in the form⁶⁰

$$\sigma(\theta) = \frac{\sigma_M}{1 + \frac{2E}{M_d c^2} \sin^2 \theta / 2} [A(q^2) + \tanh^2(\theta/2) B(q^2)], \quad (4.2)$$

where the invariant structure function $A(q^2)$ is composed of the longitudinal monopole (F_{C0}), quadrupole (F_{C2}), and transverse dipole magnetic (F_{M1}) form factors, and $B(q^2)$ is proportional to F_{M1} . In our model it can be shown that

$$A(q^2) = C_E(q^2)^2 \left[1 + \frac{2}{3} \eta (1 + \eta) \frac{M_d^2}{M^2} (\mu_p + \mu_n)^2 \right] \quad (4.3)$$

and

$$B(q^2) = C_E(q^2)^2 \frac{4}{3} \eta (1 + \eta)^2 \frac{M_d^2}{M^2} (\mu_p + \mu_n)^2, \quad (4.4)$$

where $\eta = \hbar^2 q^2 / 4M_d^2 c^2$ and

$$C_E(q^2)^2 = \left| \sum_{i=1}^{N_d} \sum_{j=1}^{N_d} (f_d^{1,i})^* f_d^{1,j} \left[\frac{4\pi}{\beta_d^i + \beta_d^j} \right]^{3/2} \times \exp[-q^2/4(\beta_d^i + \beta_d^j)] \right|^2. \quad (4.5)$$

In Figs. 2 and 3 the experimental values and the calculated curves of the invariant structure functions $A(q^2)$ and $B(q^2)$ are displayed. Using the MN interaction the MW model gives a very good description of the structure function $A(q^2)$ and reproduces $B(q^2)$ satisfactorily in the SMT region. With the BB1 and V2 interactions, on the other hand, the curves of the MW model fall off too rapidly, and the agreement with experiment is bad. In the single width models the better accord must be incidental since MW is a better approximation. At momentum transfers larger than 8 fm^{-2} even our best model fails to agree with experiment. The reason is that in this region the quadrupole component of $A(q^2)$ becomes dominant,⁶¹ and, due to the lack of the tensor force, the F_{C2} contribution is missing in $A(q^2)$ in our model. For a better agree-

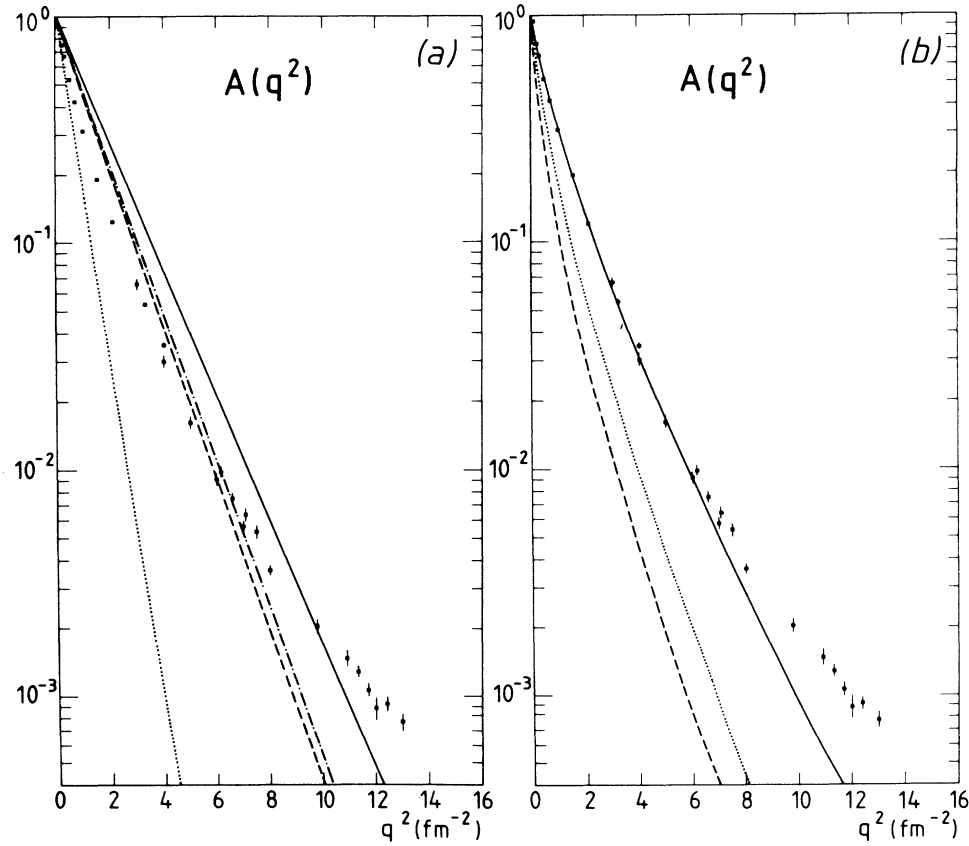


FIG. 2. The invariant structure function $A(q^2)$ of the deuteron: (a) dotted line in the CW model with force BB1, dashed-dotted line in the DW model with force BB1, solid line in the CW model with the MN force, and dashed line in the DW model with the MN force; (b) in the MW model, the solid, dashed, and dotted lines denote calculation with MN, BB1, and V2, interactions, respectively. The dots represent the data of Refs. 61–64.

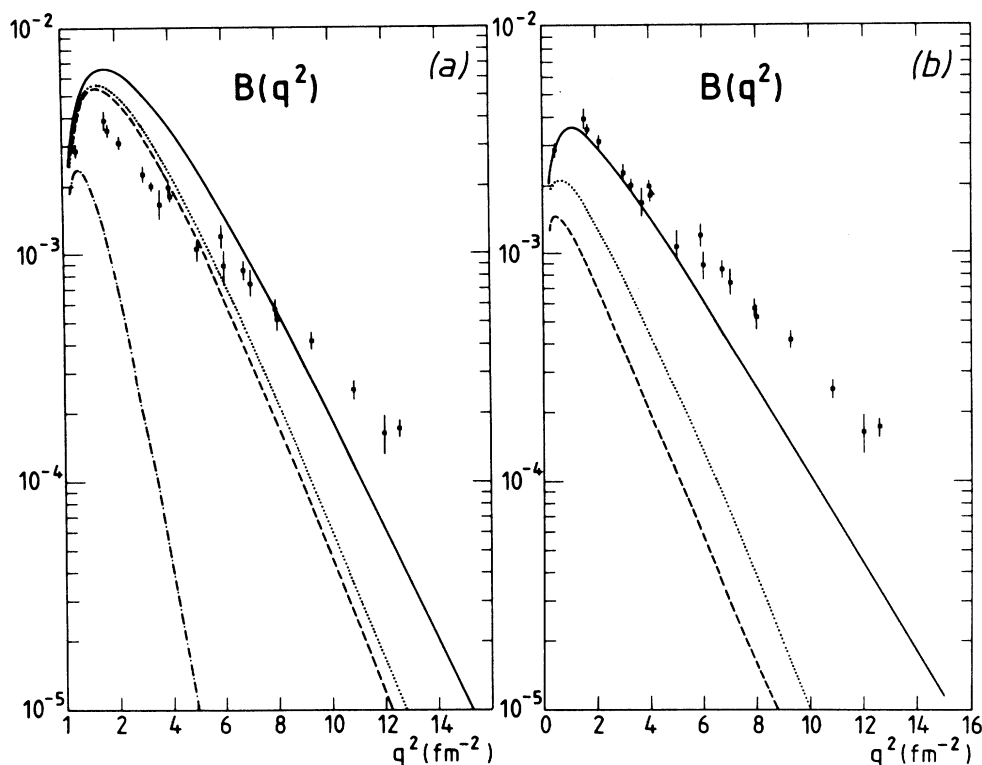


FIG. 3. The invariant structure function $B(q^2)$ of the deuteron. The notation is the same as in Fig. 2. The dots represent the data of Refs. 63–66.

ment at higher q^2 values it seems inevitable to take into account meson exchange currents and relativistic corrections.⁶⁷

B. Electromagnetic properties of ${}^6\text{Li}$ in a cluster model with breathing clusters

1. Bulk properties

For the discrete values of the width parameters in the cluster model with breathing clusters, we adopted the values that are optimal for the free clusters (Table I). The generator coordinate s was also discretized and the selected 11 points were equidistantly distributed in the interval (1 fm, 11 fm).

In the calculation of the ground state of ${}^6\text{Li}$, one exchange parameter of each interaction was adjusted (see Table III) so as to give the correct αd threshold energy (1.47 MeV). The fact that the energies of the α and d particles depend only on the combinations $W+M$ and $W+M+B+H$ gives us the chance of modifying the interactions without changing the properties of the free clusters. The reason for the adjustment is that the electromagnetic properties are sensitive to the long range part of the wave function, which depends strongly on the threshold energy. The fact that the separation energy is correct in each model makes possible a consistent comparison between different interactions and models.

In Table IV some calculated bulk properties of ${}^6\text{Li}$ are compared with the experimental values. Since for each interaction and model the alpha and deuteron separation

energies are correct, the quantitative differences in the binding energy of ${}^6\text{Li}$ derive from the ground state energies of the free clusters. A comparison between the CW and MW models with the same interaction can be found in Ref. 17. In the model $D_\alpha D_d$ the calculated rms radii of the ground state agree with the experimental value within

TABLE III. The space exchange parameters of the V2 and BB1 interactions and the u parameter of the force MN using different models. In the case of the force BB1, only its attractive part was modified.

V2	CW	0.576 79
	DW	0.457 81
	$D_\alpha D_d$	0.521 66
	$G_\alpha D_d$	0.520 32
	$G_\alpha G_d$	0.365 93
BB1	CW	0.4012
	DW	0.301 41
	$D_\alpha D_d$	0.385 67
	$G_\alpha D_d$	0.376 56
	$G_\alpha G_d$	0.148 93
MN	CW	0.925 55
	DW	0.9514
	$D_\alpha D_d$	0.9735
	$G_\alpha D_d$	0.9845
	$G_\alpha G_d$	1.3276

TABLE IV. Bulk properties of ${}^6\text{Li}$ using different models and interactions: binding energy (E), average of the energies of the first triplet 1^+ , 2^+ , and 3^+ states (E^*), rms radius of the ground state ($\langle r^2 \rangle^{1/2}$), and reduced transition strength for transition leading to the first excited state [$B(E2, 3^+ \rightarrow 1^+)$]. The experimental data are taken from Refs. 53, 54, and 68.

		E (MeV)	E^* (MeV)	$\langle r^2 \rangle^{1/2}$ (fm)	$B(E2, 3^+ \rightarrow 1^+)$ ($e^2 \text{fm}^4$)
V2	CW	-26.48	3.34	2.66	10.86
	DW	-28.85	2.25	2.78	11.65
	$D_\alpha D_d$		2.65	2.65	9.57
	$G_\alpha D_d$	-30.64	2.82	2.65	9.49
	$G_\alpha G_d$		-0.166	2.94	7.83
BB1	CW	-26.05	3.29	2.66	10.86
	DW	-28.03	2.37	2.77	10.95
	$D_\alpha D_d$		3.46	2.65	9.02
	$G_\alpha D_d$	-30.95	3.41	2.67	9.06
	$G_\alpha G_d$		-3.38	2.83	7.83
MN	CW	-25.92	3.98	2.48	7.91
	DW	-26.29	3.85	2.50	8.05
	$D_\alpha D_d$		3.60	2.50	7.69
	$G_\alpha D_d$	-27.27	3.62	2.51	7.69
	$G_\alpha G_d$		0.42	2.51	5.24
Expt.		-31.99	3.6	2.56 ± 0.1	10.9 ± 2.1

the error of the measurement for each interaction. It shows the stability of the α particle that a switching off of the distortion of α changes the rms radius of ${}^6\text{Li}$ by at most 0.02 fm. On the contrary, the neglect of the distortion of d causes a considerable increase in the rms radius in the case of the V2 and BB1 interactions. The rms radius proves to be stable as regards cluster distortions provided the MN force is used.

The calculated magnetic dipole moment of the ground state, $0.88 \mu_N$, which is model and interaction independent in our framework, compares satisfactorily with the experimental value $0.82 \mu_N$.

The wave function of the first excited state of ${}^6\text{Li}$ is also assumed to have the form (2.14), and the same set of GC's was used as in the description of the ground state, but now the relative orbital angular momentum between the clusters is taken to be 2 instead of 0. First, the same interactions were considered as in the calculation of the ground state. However, the effective forces applied do not contain spin-orbit terms and it is expected that the energy of the first excited state predicted by these models corresponds to the weighted average of the excitation energies of the first triplet 1^+ , 2^+ , and 3^+ states of ${}^6\text{Li}$. Since the inelastic electron scattering and γ decay rate are sensitive to the excitation energy, the nucleon-nucleon interactions of Table III were readjusted so as to reproduce the correct excitation energy. Two remarks concerning this readjustment should be made. First, this procedure might be considered as the simulation of the neglected spin-orbit force, and, second, because of the angular parts of the relative wave functions, the orthogonality of the ground and excited states is still held.

With the model $G_\alpha G_d$ excepted, the results concerning the excitation energy of the first excited 3^+ state of ${}^6\text{Li}$

and the reduced transition strength $B(E2, 3^+ \rightarrow 1^+)$ were obtained in fair agreement with experiment. Our results show that the α cluster remains stable but the deuteron is strongly distorted in the first excited state as well.

2. Electromagnetic form factors

The ground state charge form factors, calculated with different models and interactions, are displayed in Figs. 4 and 5. The following features can be observed. In the CW model the characteristic diffraction dip always appears, but two defects can be seen: First, the diffraction dip is not at the right position and, second, even in the SMT region there is no quantitative agreement with experiment. We see that the best result is achieved by the MN force; however, the choice of one common width parameter of the clusters is quite arbitrary, and a small change in the width parameter destroys the good agreement in the SMT region.

In the DW model the diffraction dip disappears, but at the same time in the SMT region the agreement with experiment is greatly improved. The diffraction dip disappears also in the shell model description⁵⁰ when the width parameters of the s - and p -wave orbits are chosen to be different in a particular way. Of course, in a phenomenological cluster model the different widths of the clusters can be chosen so as to obtain a good description of $|F_{C0}|^2$ including the diffraction dip. However, fitting the width parameters of the clusters to the form factor F_{C0} leads to the result³¹ that the cluster d is more extended inside ${}^6\text{Li}$ than the free deuteron. This is in contrast to the results of the dynamical calculations, which predict the shrinking of the deuteron^{14,17,23,71} and thus seems unphysical. We have adopted the viewpoint of the dynamical

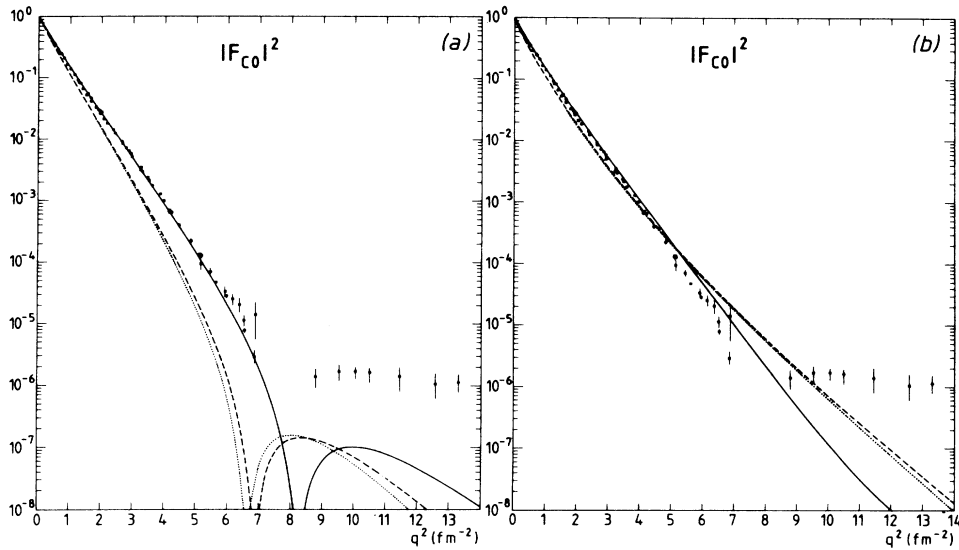


FIG. 4. Squared charge form factor of the ground state of ${}^6\text{Li}$: (a) in the CW model, (b) in the DW model. The solid, dashed, and dotted lines denote calculations with the MN, V2, and BB1 interactions, respectively. The dots represent the data of Refs. 69 and 70.

cluster models, and want to carry it through with all its implications.

The $D_\alpha D_d$ model can record a remarkable success by reproducing $|F_{C0}|^2$ in the SMT region. In the following we shall give an account of the tests carried out to establish the cause of its failure to reproduce the diffraction dip.

We tested the forces against another one optimized to our $D_\alpha D_d$ model.⁷² This force gives virtually exact binding energies and rms radii for the nuclei ${}^2\text{H}$, ${}^3\text{H}$, ${}^3\text{He}$, and ${}^4\text{He}$, reproduces the experimental binding energy of ${}^6\text{Li}$, and, in addition, predicts the binding energies of the other

nuclei of two s -wave clusters, viz., ${}^5\text{He}$, ${}^5\text{Li}$, ${}^7\text{Li}$, ${}^7\text{Be}$, and ${}^8\text{Be}$, with an accuracy of 1 MeV. This force produced no diffraction dip of $|F_{C0}|^2$ either.

It was observed that using fewer cluster width parameters, for example, one for α and two for d as in Ref. 23, the diffraction dip reappears. The position of the diffraction minimum is very sensitive to the values of the widths. Using the interaction and width parameters given in Ref. 23, the minimum is obtained around 8.5 fm^{-2} , but when the cluster stability condition is imposed the dip is shifted to a considerably higher q^2 values (11.3 fm^{-2}). However, as we have seen, a proper description of α and

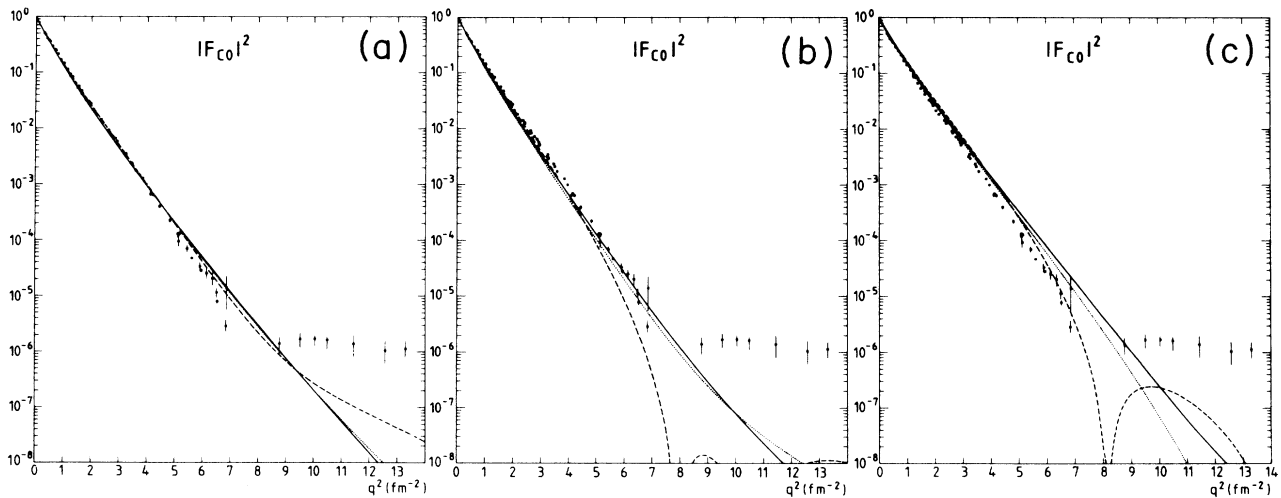


FIG. 5. Squared charge form factor of the ground state of ${}^6\text{Li}$ in the MW model: (a) with the V2 force, (b) with the BB1 force, and (c) with the MN force. The solid, dashed, and dotted lines denote the results of the $D_\alpha D_d$, $G_\alpha G_d$, and $G_\alpha D_d$ models, respectively. The dots represent the data of Refs. 69 and 70.

d requires more width parameters, and a corresponding extension of the model space for ${}^6\text{Li}$ invariably causes the diffraction minimum to disappear.

A qualitative analysis of the form factor may be implemented by neglecting the intercluster antisymmetrization. In this approximation F_{C0} reduces to

$$F_{C0}(q) = \frac{2}{3}F_{ad}(\frac{1}{3}q)F_{\alpha}(q) + \frac{1}{3}F_{ad}(\frac{2}{3}q)F_d(q), \quad (4.6)$$

where $F_{\alpha}(q)$ and $F_d(q)$ are the charge form factors of the clusters α and d , respectively, and $F_{ad}(q)$ is the Fourier transform of the wave function of the relative motion of the clusters. In our models the presence of the diffraction dip may be explained in the following way. The wave function of the relative motion that can be used in a nonantisymmetrized model looks like a $2s$ -type harmonic oscillator wave function. The Fourier transform of a relative function of this type has both positive and negative parts. In the CW, DW, and $G_{\alpha}G_d$ models the possible diffraction dip of $|F_{C0}(q)|^2$ can only be attributed to the relative motion since, on one hand, according to Eq. (4.1), the form factors of the clusters are positive everywhere when each cluster is described by one width parameter, and, on the other hand, in the MW model of α and d the sign change in the form factors $F_{\alpha}(q)$ and $F_d(q)$ are at q^2 values much higher than the minimum of the squared form factor of ${}^6\text{Li}$.

This picture becomes more complicated in the $D_{\alpha}D_d$, $G_{\alpha}D_d$, and $D_{\alpha}G_d$ models because of interference with the form factors of the cluster excited states. The effect of these extra terms may be interpreted by saying that the dip due to the relative motion is shifted away and that the separate clusters are not brought down sufficiently for ${}^6\text{Li}$. Thus the diffraction dip of ${}^6\text{Li}$ can be derived neither from those present in the models of the separate clusters nor from that of the relative motion. However, the actual ex-

perimental $|F_{C0}(q)|^2$ of the α particle does contain a diffraction dip almost coinciding with that of ${}^6\text{Li}$. Our analysis thus strongly indicates that the latter could only be derived from the former. It has been proposed that the diffraction minimum of the form factor of α can only be explained by introducing Jastrow correlation into the wave function. Thus our conclusion is that in the understanding of the ground state charge form factor of ${}^6\text{Li}$ the short range NN correlation must play a substantial role. Our study of the αd fragmentation strength also points to some missing short range correlation.⁷²

However, careful analyses have to be carried out since the region of the dip of the squared charge form factor of ${}^6\text{Li}$ is just the momentum transfer area where the non-nucleonic degrees of freedom come in to play. For example, the meson exchange currents may help to explain the second maximum of the squared form factor of ${}^6\text{Li}$.⁷³

Now let us turn to the study of the cluster distortions. In Fig. 5 the calculated charge form factors of the $D_{\alpha}D_d$, $G_{\alpha}D_d$, and $G_{\alpha}G_d$ models are shown. Both the alpha and deuteron distortions have an effect on the shape of the charge form factor only in high momentum transfer regions ($q^2 > 8 \text{ fm}^{-2}$), but the former to a lesser extent.

Our results show that the good agreement with experiment in the SMT region is a consequence of using realistic ground states of the clusters.

The calculated charge density $\rho(r)$ of the ground state is shown in Figs. 6 and 7, together with the experimentally fitted charge density distribution of Li *et al.*⁷⁰ that contains six adjustable parameters. Using the CW model the calculated curves of $\rho(r)$ deviate badly from the fitted one. The charge density of the central region is considerably underestimated using the V2 and BB1 forces and is overshoot using the MN interaction. Whichever interaction is used, the distortion enhances the charge density in the vicinity of the origin. With the model $D_{\alpha}D_d$ used, the

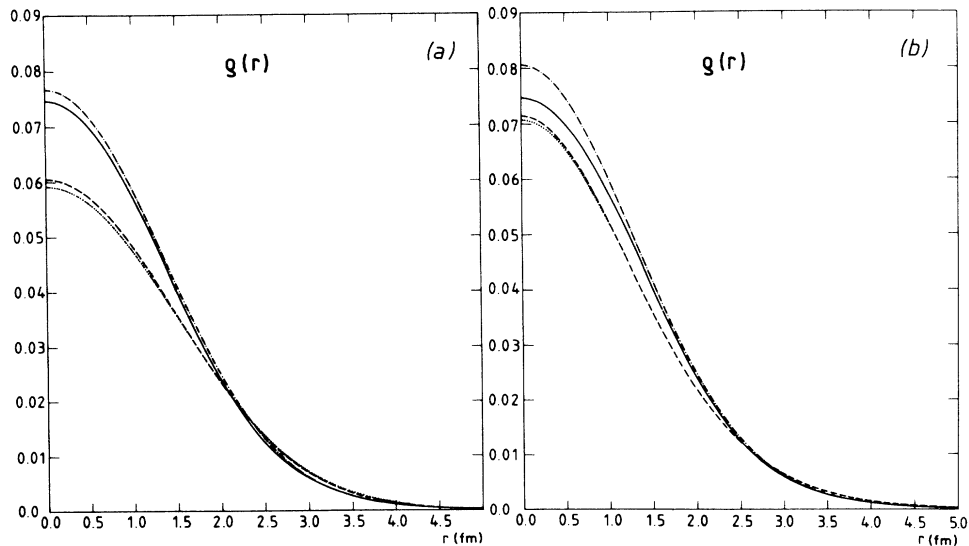


FIG. 6. Charge density of the ground state of ${}^6\text{Li}$: (a) in the CW model, (b) in the DW model. The solid line represents the charge density of Li *et al.* (Ref. 70) fitted to the experiment. The dashed, dotted, and dashed-dotted lines denote the result of the calculation with the V2, BB1, and MN interactions, respectively.

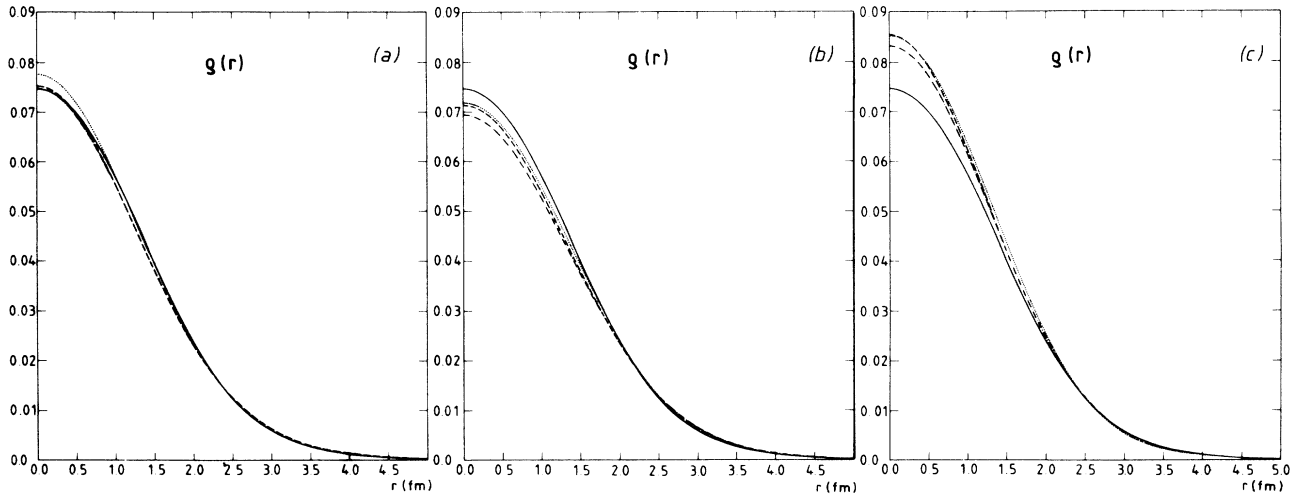


FIG. 7. Charge density of the ground state of ${}^6\text{Li}$ in the MW model: (a) with the V2 force, (b) with the BB1 force, and (c) with the MN force. The solid line represents the density of Li *et al.* (Ref. 70) fitted to the experiment. The dashed, dotted, and dashed-dotted lines denote the result of the $D_\alpha D_d$, $G_\alpha D_d$, and $G_\alpha G_d$ models, respectively.

calculated charge densities are close to the phenomenological one when V2 or BB1 interactions are used, but the value remains too large at the center in the case of the MN force. It was observed in cluster and shell model studies that short range NN correlations through a Jastrow function depress the charge density around the center but enhance it in the region between 2 and 4 fm.^{7,9,33} These are the very areas where our calculated charge densities are not in agreement with the experimentally fitted curve. Thus it may be hoped that with Jastrow correlation the high momentum behavior of the charge form factor of the cluster model with breathing clusters

can also be improved.

The calculated squared inelastic charge form factor $|F_{C_2}^*(q)|^2$ of the excitation of the 2.18 MeV state is presented in Figs. 8 and 9. The results of the CW model in each case are in quite good agreement with the experimental data. Although the introduction of different width parameters for the clusters makes the results worse, especially beyond the maximum of the squared form factor $|F_{C_2}^*|^2$, the inelastic charge form factor of the model $D_\alpha D_d$ reproduces the measured values very well. It is remarkable that here the maximum in $|F_{C_2}^*|^2$, usually described unsatisfactorily,^{11,78} is predicted in good agree-

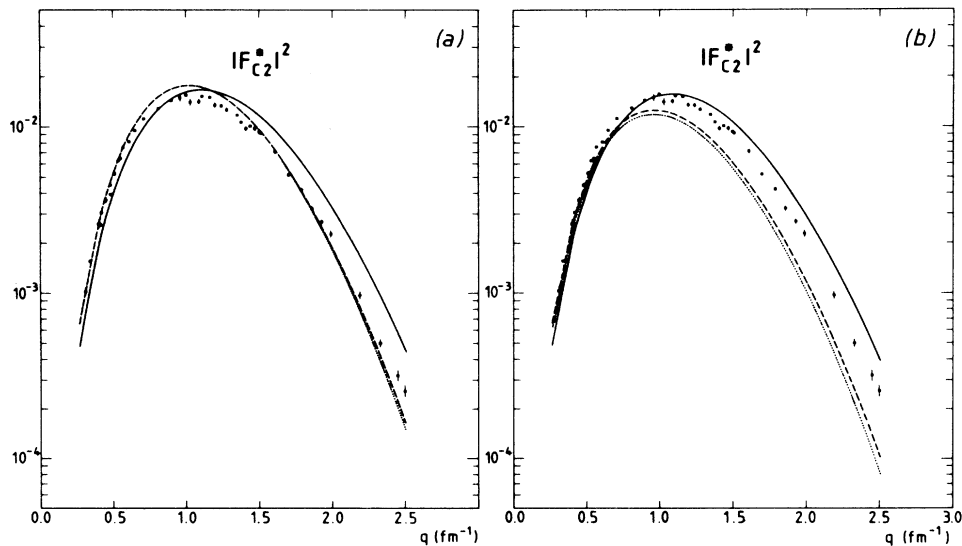


FIG. 8. Squared inelastic charge form factor of ${}^6\text{Li}$: (a) in the CW model, (b) in the DW model. The solid, dashed, and dotted lines denote calculations with the MN, V2, and BB1 interactions, respectively. The dots represent the data of Refs. 74–77.

ment with experiment.

The stability of the α cluster is nicely demonstrated in the model calculations $G_\alpha D_d$. In Fig. 9 the difference between the curves of $|F_{C2}^*|^2$ calculated with the models $D_\alpha D_d$ and $G_\alpha D_d$ is unobservable for each interaction. According to the calculation with the $G_\alpha G_d$ model, the distortion of the d cluster greatly influences the shape of the squared inelastic charge form factor even at very small momentum transfer.

For the magnetic form factor of the ground state of ${}^6\text{Li}$, our calculation is the first in a dynamical microscopic cluster model. Our calculated elastic transverse form factor of ${}^6\text{Li}$ and the measured data are depicted in Figs. 10 and 11. The rough shape of the magnetic dipole form factor $|F_{M1}|^2$ is reproduced by each model and interaction considered. Using the V2 or BB1 force the diffraction minimum of $|F_{M1}|^2$ was predicted at too small momentum transfer and after the first maximum of $|F_{M1}|^2$ the calculated curves deviate significantly from the measured values. However, the MN interaction produces nice agreement with experiment over the whole region of measured momentum transfer. The good result gained with the MN force may be attributed to the proper description of the deuteron since the magnetic form factor of ${}^6\text{Li}$ depends mainly on the nucleons of the deuteron cluster. The effect of the breathing excited states of α on the form factor $|F_{M1}|^2$ is almost unobservable in Fig. 11. The breathing states of d, on the contrary, markedly influence the behavior of $|F_{M1}|^2$ around its second maximum and shift the minimum of $|F_{M1}|^2$.

Simultaneous description of the longitudinal and transverse form factors of ${}^6\text{Li}$ has not been successful, neither in terms of a three-body model¹⁶ nor standard phenomenological cluster models.^{31,32} Our results show that, using dynamically determined wave functions in a microscopic cluster model with breathing clusters and a realistic interaction, all form factors F_{C0} , F_{M1} , and F_{C2}^* can be obtained with good accuracy in the SMT region.

V. SUMMARY

The effect of the breathing excited states of the deuteron and alpha clusters on the electromagnetic properties of ${}^6\text{Li}$ was examined using a GC-type cluster model of ${}^6\text{Li}$. It should be emphasized that the calculations are free from the spurious center-of-mass motion and arbitrary parameters. The oscillator width parameters of the clusters and the exchange mixtures of the NN interaction were determined by the cluster stability condition and by the correct separation energy value, respectively. In order to see the force dependence, the calculations were carried out with three different central interactions. The following conclusions are found to be general, independent of the force.

It was found that at low momentum transfer ($q^2 < 8 \text{ fm}^{-2}$) the charge form factor of the ground state of ${}^6\text{Li}$ was modified very slightly by mixing the breathing excited states of the clusters into the wave function. What is important in the low- q^2 region is the quality of the ground states of the clusters. With a realistic ground state of the deuteron, the monopole charge form factor of ${}^6\text{Li}$ is reproduced excellently in the low- q^2 region. On the other hand, around and beyond the diffraction dip the shape of the squared charge form factor is greatly influenced by the breathing excited states of the deuteron.

An unexpected by-product of the increase of the model space by including more and more breathing excited states of the clusters into the wave function is the gradual disappearance of the experimentally observed diffraction minimum of the squared charge form factor $|F_{C0}(q)|^2$. As the extension of the model space is bound to improve the wave function for a fixed Hamiltonian, this deficiency most probably reflects the important role played by the neglected non-nucleonic degrees of freedom in this momentum transfer region. These non-nucleonic degrees of freedom manifest themselves partly in the repulsive core of the effective NN interaction. However, our

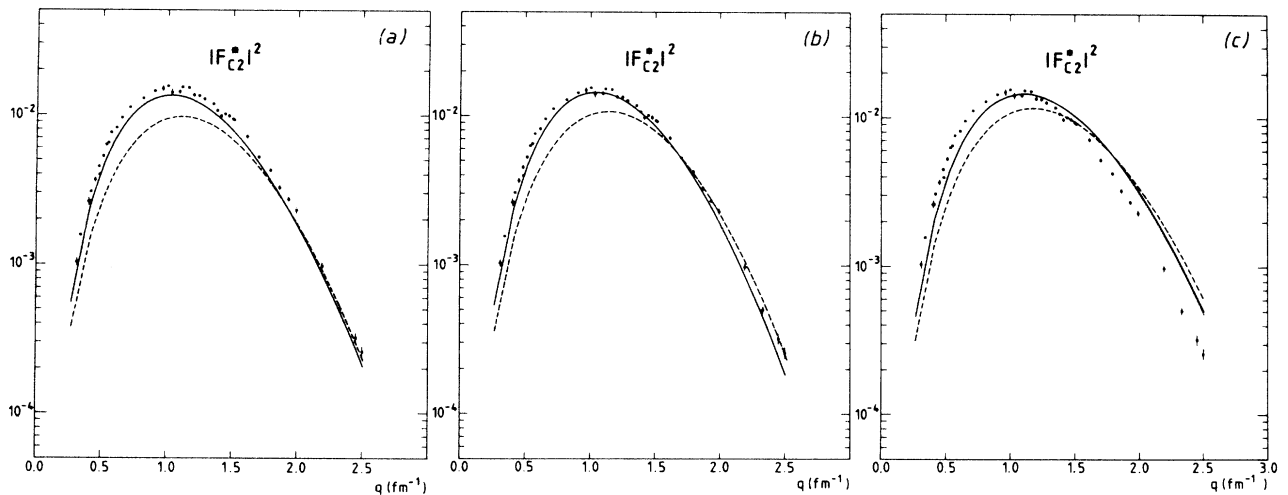


FIG. 9. Squared inelastic charge form factor of ${}^6\text{Li}$ in the MW model: (a) with the V2 force, (b) with the BB1 force, and (c) with the MN force. The solid, dashed, and dotted lines denote the results of the $D_\alpha D_d$, $G_\alpha G_d$, and $G_\alpha D_d$ models, respectively. The curves of the $D_\alpha D_d$ and $G_\alpha D_d$ models coincide in (a) and (b). The dots represent the data of Refs. 74–77.

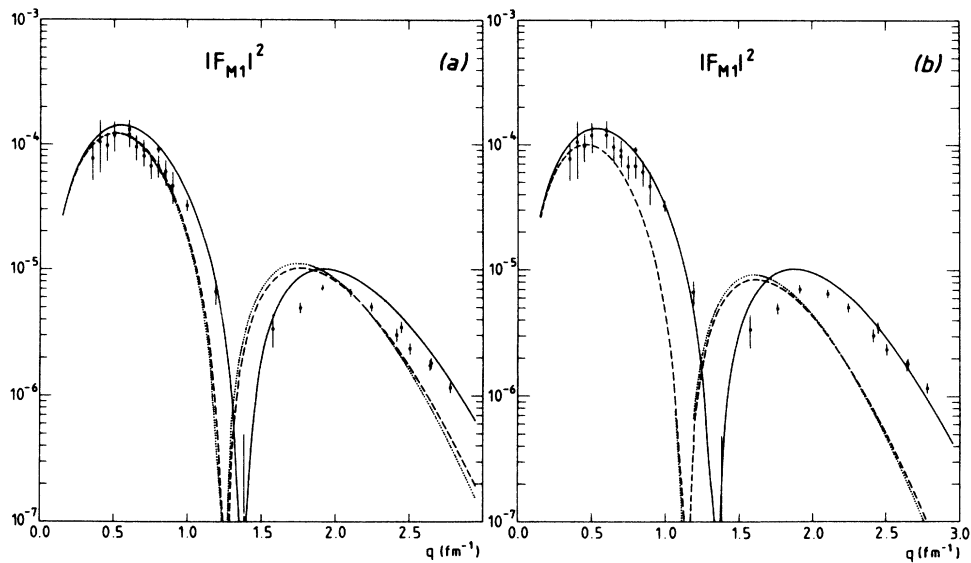


FIG. 10. Squared magnetic form factor of the ground state of ${}^6\text{Li}$: (a) in the CW model, (b) in the DW model. The solid, dashed, and dotted lines denote calculations with the MN, V2, and BB1 interactions, respectively. The dots represent the data of Ref. 32.

effective NN interactions contain only repulsive cores of modest strength. It would be desirable to use more saturating NN interactions, but in that case Jastrow correlation functions are to be used. Jastrow factors could be introduced into the breathing cluster model, but, unfortunately, the calculation would be extremely difficult and laborious because relative coordinates should be applied from the onset, and so one of the main advantages of the GC method, namely the possibility of using Slater determinants, would be lost. At any rate, the short range NN correlation was shown to be very important in the explanation of the diffraction dip of ${}^6\text{Li}$ in shell model

descriptions^{6,7,9,73} as well. To get quantitative agreement in the high momentum transfer region, other effects also have to be taken into account explicitly, e.g., the usual underestimation of the second maximum of the squared charge form factor can be partly remedied by considering meson exchange currents.

The transverse form factor of the ground state of ${}^6\text{Li}$ had not been studied earlier with dynamical microscopic cluster models. Our results showed that the magnetic dipole and charge form factors of the ground state can be well described simultaneously using the same variationally determined wave function. The rough shape of the mag-

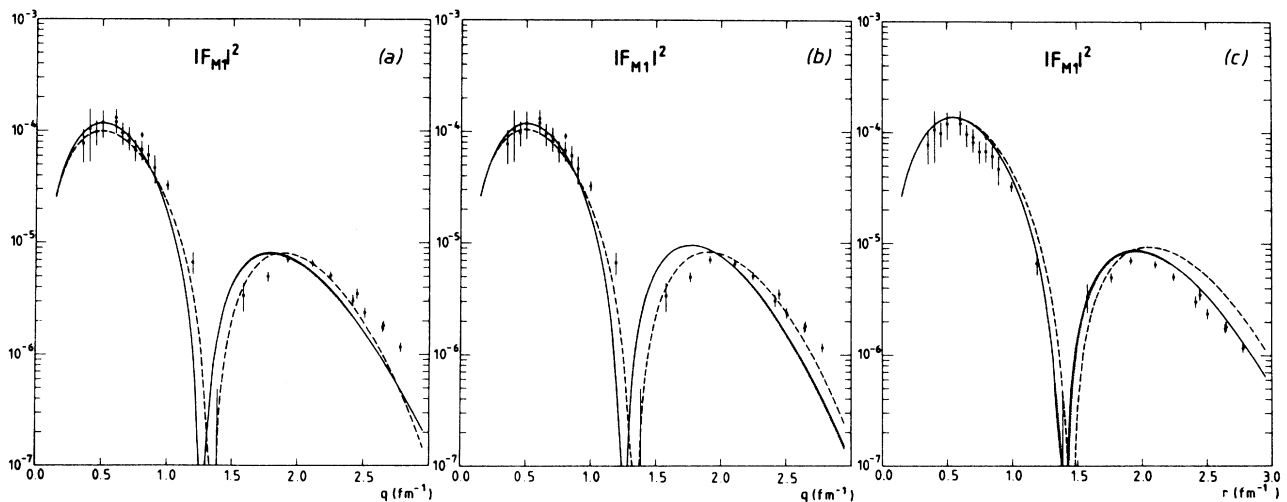


FIG. 11. Squared magnetic form factor of the ground state of ${}^6\text{Li}$ in the MW model: (a) with the V2 force, (b) with the BB1 force, and (c) with the MN force. The solid, dashed, and dotted lines denote the results of the $D_a D_d$, $G_a G_d$, and $G_a D_d$ models, respectively. The dots represent the data of Ref. 32.

netic form factor was reproduced with each model and interaction used. However, good agreement over the whole experimentally measured region was only reached by using an interaction which properly describes the deuteron (e.g., the Minnesota force). The excited states of the cluster d affect the position of the diffraction minimum of $|F_{M1}(q)|^2$ and its shape around the second maximum.

The influence of the breathing excited states of d on the squared inelastic charge quadrupole form factor $|F_{C2}^*(q)|^2$ is shown to be very important. The shape of the squared form factor $|F_{C2}^*(q)|^2$ below and around its first maximum is reproduced only with the inclusion of the breathing excited states of d . The predicted curve of $|F_{C2}^*(q)|^2$ is in very good agreement with the measurement. The effect of the excited states of d on $|F_{C2}^*(q)|^2$ is larger than on $|F_{C0}(q)|^2$; it is considerable even in the low- q^2 region. This can be explained by assuming it is more probable to find excited d configurations in an excited state than in the ground state of ${}^6\text{Li}$.

The stability of the α particle was demonstrated in a number of cluster model calculations for α scattering. Our results also indicate the rigidity of the α cluster. In the calculations of the form factors $|F_{C0}(q)|^2$, $|F_{M1}(q)|^2$, and $|F_{C2}^*(q)|^2$, the breathing excited states of α can be neglected, at least at small momentum transfer,

but even the distortion of the cluster α can be observed in the high q^2 region.

All in all, the cluster model with breathing clusters was shown to be able to give a very good simultaneous description of the elastic and inelastic charge form factors and the elastic magnetic form factor in the low- q^2 region. However, in order to clarify the discrepancy found in the high momentum behavior of the form factor $|F_{C0}|^2$ and to describe the quadrupole moment of the ground state, our model has to be improved in two respects: First, the flexibility of the wave function has to be increased by employing correlation functions of the Jastrow type to reckon with the short range NN correlation, and, second, the central NN interaction has to be replaced by a more realistic one containing spin-orbit and tensor components.

ACKNOWLEDGMENTS

One of us (A.T.K.) wishes to thank Prof. G. Schatz and the Kernforschungszentrum Karlsruhe for their kind hospitality, and Prof. A. Faessler and Dr. R. G. Lovas for useful discussions. A.T.K. is indebted to Prof. R. Neuhausen for providing him with the magnetic form factor data of Dr. L. Lapikás. This work was partially supported by the Soros Foundation, New York.

*Deceased.

¹G. R. Bureson and R. Hofstadter, Phys. Rev. **112**, 1282 (1958).

²L. R. B. Elton, *Nuclear Sizes* (Oxford University Press, Oxford, 1961).

³D. F. Jackson, Proc. Phys. Soc. London **76**, 949 (1960).

⁴M. A. K. Lodhi, Nucl. Phys. **80**, 125 (1966).

⁵L. R. B. Elton and M. A. K. Lodhi, Nucl. Phys. **66**, 209 (1965).

⁶S. S. M. Wong and D. L. Lin, Nucl. Phys. **A101**, 663 (1967).

⁷C. Ciofi degli Atti and N. M. Kabachnik, Phys. Rev. C **1**, 809 (1970).

⁸D. A. Sparrow and W. J. Gerace, Nucl. Phys. **A145**, 289 (1969).

⁹C. Ciofi degli Atti, Nucl. Phys. **A129**, 350 (1969).

¹⁰M. A. K. Lodhi, Phys. Rev. C **3**, 503 (1971).

¹¹G. L. Payne and B. P. Nigam, Phys. Rev. C **21**, 1177 (1979).

¹²K. Wildermuth and Y. C. Tang, *A Unified Theory of the Nucleus* (Academic, New York, 1977).

¹³R. Krivec and M. V. Mihailovic, J. Phys. G **8**, 821 (1982).

¹⁴R. Beck, F. Dickmann, and R. G. Lovas, Ann. Phys. (N.Y.) **173**, 1 (1987).

¹⁵J. Bang and C. Gignoux, Nucl. Phys. **A313**, 119 (1979).

¹⁶V. I. Kukulín, V. M. Krasnopol'sky, V. T. Voronchev, and P. B. Sazanov, Nucl. Phys. **A417**, 128 (1984).

¹⁷R. Beck, F. Dickmann, and A. T. Kruppa, Phys. Rev. C **30**, 1044 (1984).

¹⁸D. R. Thompson and Y. C. Tang, Phys. Rev. **179**, 971 (1969).

¹⁹H. Jacobs, K. Wildermuth, and E. J. Wurster, Phys. Lett. **29B**, 455 (1969).

²⁰D. R. Thompson and Y. C. Tang, Phys. Rev. C **8**, 1649 (1973).

²¹D. R. Thompson, Y. C. Tang, and F. S. Chwieroth, Phys. Rev. C **10**, 987 (1974).

²²H. Kanada, T. Kaneko, H. Nishioka, and S. Saito, Prog.

Phys. **63**, 842 (1980).

²³H. Kanada, T. Kaneko, and Y. C. Tang, Nucl. Phys. **A389**, 285 (1982).

²⁴H. Kanada, T. Kaneko, M. Nomoto, and Y. C. Tang, Prog. Theor. Phys. **72**, 369 (1984).

²⁵H. Kanada, T. Kaneko, S. Saito, and Y. C. Tang, Nucl. Phys. **A444**, 209 (1985).

²⁶Yu. A. Kuderyarov, Yu. F. Smirnov, and M. A. Chebotarev, Yad. Fiz. **4**, 1048 (1966) [Sov. J. Nucl. Phys. **4**, 751 (1967)].

²⁷V. G. Neudatchin and Yu. F. Smirnov, Prog. Nucl. Phys. **10**, 275 (1969).

²⁸Il-T. Cheon, Phys. Lett. **30B**, 81 (1969).

²⁹A. K. Jain and N. Sarma, Phys. Lett. **33B**, 271 (1970).

³⁰Yu. A. Kuderyarov, I. V. Kurdyumov, V. G. Neudatchin, and Yu. F. Smirnov, Nucl. Phys. **A163**, 316 (1971).

³¹J. C. Bergstrom, Nucl. Phys. **A327**, 458 (1979).

³²J. C. Bergstrom, S. B. Kowalski, and R. Neuhausen, Phys. Rev. C **25**, 1156 (1982).

³³E. W. Schmid, Y. C. Tang, and K. Wildermuth, Phys. Lett. **7**, 263 (1963).

³⁴J. M. Hansteen and H. W. Wittern, Phys. Lett. **24B**, 381 (1967).

³⁵H. Stowe, H. H. Hackenbroich, and H. Hutzelmeyer, Z. Phys. **247**, 95 (1971).

³⁶A. Hasegawa and S. Nagata, Prog. Theor. Phys. **45**, 1786 (1971).

³⁷T. Mertelmeier and H. M. Hofmann, Nucl. Phys. **A459**, 387 (1986).

³⁸T. Kajino, T. Matsuse, and A. Arima, Nucl. Phys. **A413**, 323 (1984).

³⁹T. Kajino, T. Matsuse, and A. Arima, Nucl. Phys. **A414**, 185 (1984).

⁴⁰Y. C. Tang, in *Topics in Nuclear Physics*, edited by T. T. S. Kuo and S. S. M. Wong (Springer-Verlag, Berlin, 1981), Vol.

- 2, p. 572.
- ⁴¹M. A. Nagarajan and R. G. Lovas, Daresbury Laboratory Report DL/NUC/P107T/1980, 1980.
- ⁴²A. B. Volkov, Nucl. Phys. **74**, 33 (1965).
- ⁴³D. M. Brink and E. Boeker, Nucl. Phys. **A91**, 1 (1967).
- ⁴⁴D. R. Thompson, M. LeMere, and Y. C. Tang, Nucl. Phys. **A286**, 53 (1977).
- ⁴⁵K. F. Pál *et al.*, Nucl. Phys. **A402**, 114 (1983).
- ⁴⁶R. S. Willey, Nucl. Phys. **40**, 529 (1963).
- ⁴⁷T. DeForest, Jr. and J. D. Walecka, Adv. Phys. **15**, 1 (1966).
- ⁴⁸H. Uberall, *Electron Scattering from Complex Nuclei* (Academic, New York, 1971).
- ⁴⁹C. Ciofi degli Atti, Prog. Part. Nucl. Phys. **3**, 163 (1980).
- ⁵⁰M. Bouten and M. C. Bouten, J. Phys. G **8**, 1641 (1982).
- ⁵¹L. Tassie and F. Barker, Phys. Rev. **111**, 940 (1958).
- ⁵²H. Kanada, O. K. K. Liu, and Y. C. Tang, Phys. Rev. C **22**, 813 (1980).
- ⁵³A. H. Wapstra and N. B. Gove, Nucl. Data Tables **9**, 265 (1971).
- ⁵⁴R. C. Barrett and D. F. Jackson, *Nuclear Sizes and Structure* (Clarendon, Oxford, 1977).
- ⁵⁵T. Vertse, K. F. Pál, and Z. Balogh, Comput. Phys. Commun. **27**, 309 (1982).
- ⁵⁶R. F. Frosch, J. S. McCarthy, R. E. Rand, and M. R. Yearian, Phys. Rev. **160**, 874 (1967).
- ⁵⁷W. Czyz and L. Lesniak, Phys. Lett. **25B**, 319 (1967).
- ⁵⁸J. Borysowicz and D. O. Riska, Nucl. Phys. **A254**, 301 (1975).
- ⁵⁹M. Radomski and D. O. Riska, Nucl. Phys. **A274**, 428 (1976).
- ⁶⁰V. M. Muzafarov and V. E. Troitskii, Yad. Fiz. **33**, 1461 (1981) [Sov. J. Nucl. Phys. **33**, 783 (1981)].
- ⁶¹S. Galster *et al.*, Nucl. Phys. **B32**, 221 (1971).
- ⁶²C. D. Buchanan and M. R. Yearian, Phys. Rev. Lett. **15**, 303 (1965).
- ⁶³D. Benekas, D. Drickey, and D. Frerejacque, Phys. Rev. **148**, 1327 (1966).
- ⁶⁴G. G. Simon, Ch. Schmitt, and V. H. Walter, Nucl. Phys. **A364**, 285 (1981).
- ⁶⁵D. Ganichot, B. Grossetete, and D. B. Isabelle, Nucl. Phys. **A178**, 545 (1972).
- ⁶⁶S. Auffret *et al.*, Phys. Rev. Lett. **54**, 649 (1985).
- ⁶⁷V. M. Muzafarov, V. E. Troitskii, and S. V. Trubnikov, Fiz. Elem. Chastits. At. Yadra **14**, 1112 (1983) [Sov. J. Part. Nucl. **14**, 467 (1983)].
- ⁶⁸F. Ajzenberg-Selove, Nucl. Phys. **A413**, 1 (1984).
- ⁶⁹L. R. Suelzle, M. R. Yearian, and H. Crannel, Phys. Rev. **162**, 992 (1967).
- ⁷⁰G. C. Li, I. Sick, R. R. Whitney, and M. R. Yearian, Nucl. Phys. **A162**, 583 (1971).
- ⁷¹R. E. Brown and Y. C. Tang, Phys. Rev. **176**, 1235 (1968).
- ⁷²A. T. Kruppa, R. G. Lovas, R. Beck, and F. Dickmann, Phys. Lett. **179B**, 317 (1986).
- ⁷³M. A. K. Lodhi and R. B. Hamilton, Phys. Rev. Lett. **54**, 646 (1984).
- ⁷⁴F. Eigenbrod, Z. Phys. **228**, 337 (1969).
- ⁷⁵R. Yen *et al.*, Nucl. Phys. **A235**, 135 (1974).
- ⁷⁶J. C. Bergstrom and E. L. Tomusiak, Nucl. Phys. **A262**, 196 (1976).
- ⁷⁷J. C. Bergstrom, U. Deutschmann, and R. Neuhausen, Nucl. Phys. **A327**, 439 (1979).
- ⁷⁸Il-T. Cheon, S. J. Choi, and M. T. Jeong, Phys. Lett. **144B**, 312 (1984).